Single Membrane Reactor Configuration for Separation of Hydrogen, Carbon Dioxide and Hydrogen Sulfide

Final Technical Report

Reporting Period Start Date: 6/01/2005

Reporting Period End Date: 5/31/2008

Principal Authors:

Michael Roberts, Robert Zabransky, Shain Doong*, and Jerry Lin**

*UOP LLC
** Arizona State University

Date Report Issued: August 2008

DOE Award Number: DE-FC26-05NT42450

Submitting Organization:

Gas Technology Institute
1700 South Mount Prospect Road
Des Plaines, IL 60018

Subcontractor
Department of Chemical Engineering
Arizona State University
Tempe, AZ 85287

DISCLAIMER

ABSTRACT

The objective of the project was to develop a novel complementary membrane reactor process that can consolidate two or more downstream unit operations of a coal gasification system into a single module for production of a pure stream of hydrogen and a pure stream of carbon dioxide. The overall goals were to achieve higher hydrogen production efficiencies, lower capital costs and a smaller overall footprint than what could be achieved by utilizing separate components for each required unit process/operation in conventional coal-to-hydrogen systems.

Specifically, this project was to develop a novel membrane reactor process that combines hydrogen sulfide removal, hydrogen separation, carbon dioxide separation and water-gas shift reaction into a single membrane configuration. The carbon monoxide conversion of the water-gas-shift reaction from the coal-derived syngas stream is enhanced by the complementary use of two membranes within a single reactor to separate hydrogen and carbon dioxide. Consequently, hydrogen production efficiency is increased. The single membrane reactor configuration produces a pure H_2 product and a pure CO_2 permeate stream that is ready for sequestration. This project focused on developing a new class of CO_2-selective membranes for this new process concept.

Several approaches to make CO_2-selective membranes for high-temperature applications have been tested. Membrane disks using the technique of powder pressing and high temperature sintering were successfully fabricated. The powders were either metal oxide or metal carbonate materials. Experiments on CO_2 permeation testing were also performed in the temperature range of 790º to 940°C for the metal carbonate membrane disks. However, no CO_2 permeation rate could be measured, probably due to very slow CO_2 diffusion in the solid state carbonates.

To improve the permeation of CO_2, one approach is to make membranes containing liquid or molten carbonates. Several different types of dual-phase membranes were fabricated and tested for their CO_2 permeation in reducing conditions without the presence of oxygen. Although the flux was quite low, on the order of 0.01-0.001 cc STP/cm^2/min, the selectivity of CO_2/He was almost infinite at temperatures of about 800°C.

A different type of dual-phase membrane prepared by Arizona State University (ASU) was also tested at GTI for CO_2 permeation. The measured CO_2 fluxes were 0.015 and 0.02 cc STP/cm^2/min at 750 and 830 °C, respectively. These fluxes were higher than the previous flux obtained (~0.01 cc STP/cm^2/min) using the dual-phase membranes prepared by GTI. Further development in membrane development should be conducted to improve the CO_2 flux.

ASU has also focused on high temperature permeation/separation experiments to confirm the carbon dioxide separation capabilities of the dual-phase membranes with $La_{0.6}Sr_{0.4}Co_{0.8}Fe_{0.2}O_{3-\delta}$ (LSCF6482) supports infiltrated with a Li/Na/K molten carbonate mixture (42.5/32.5/25.0 mole %). The permeation experiments indicated that the addition of O_2 does improve the permeance of CO_2 through the membrane.

A simplified membrane reactor model was developed to evaluate the performance of the process. However, the simplified model did not allow the estimation of membrane transport area, an important parameter for evaluating the feasibility of the proposed membrane reactor technology. As a result, an improved model was developed. Results of the improved membrane reactor model show that the membrane shift reaction has promise as a means to simplify the production of a clean stream of hydrogen and a clean stream of carbon dioxide. The focus of additional development work should address the large area required for the CO_2 membrane as identified in the modeling calculations.

Also, a more detailed process flow diagram should be developed that includes integration of cooling and preheating feed streams as well as particulate removal so that steam and power generation could be optimized.

For the tubular membranes that were fabricated by solution impregnation with metal carbonates, difficulties were encountered in removing the impurity salts that were trapped inside the porous support tube. The membrane tube would continue losing weight even after being heated up to 500 °C in air and could not maintain its nonporous characteristics. This approach was therefore abandoned.
Dual-phase membranes with molten carbonates were subsequently shown to have CO_2 permeability in reducing conditions without the presence of oxygen; they were also tested for H_2S permeation. Permeation tests were conducted with a gas feed composition consisting of 33.6% CO_2, 8.4% He, 57.6% H_2 and 0.4% H_2S at temperatures between 820º and 850 °C and a pressure of 1 bar. On the permeate side, hydrogen was used as a sweep gas to react with any sulfide ion that permeated through the membrane to form H_2S. The measured H_2S flux was on the order of 0.01-0.03 cc STP/cm^2/min. The flux of H_2S was considerably higher than that of CO_2, with a H_2S/CO_2 selectivity approaching 2,000. This type of membrane can be used for the front end sulfur removal in the single membrane reactor configuration.

In the area of hydrogen transport membranes, the palladium-copper (Pd-Cu) alloy membrane was selected over the proton-conducting ceramic membrane for the hydrogen separation section of the single membrane reactor configuration. However, the metallic membrane should be evaluated for its thermal stability in the temperature range of interest in this project, 750°-900°C. The other issue is sulfur tolerance of the metallic membrane. In general, high temperature operation should be more favorable in terms of sulfur resistance. Hydrogen permeation of a commercial Pd-Cu alloy foil was tested at 850°C continuously for about 2 weeks. There was no performance degradation observed relative to hydrogen flux, which is a good indication of its thermal stability at this high temperature. A permeation test was also performed with a feed gas containing 1000 ppm H_2S, 50% H_2(by volume), balance He at 850 °C. No hydrogen flux decline was observed after 8 hours of operation, indicating a good sulfur resistance for this material.

TABLE OF CONTENTS

LIST OF GRAPHICAL MATERIALS

Figure No.

LIST OF TABLES

EXECUTIVE SUMMARY

The objective of the project was to develop a novel complementary membrane reactor process that can consolidate two or more downstream unit operations of a coal gasification system into a single module for production of a pure stream of hydrogen and a pure stream of carbon dioxide. The overall goals were to achieve higher hydrogen production efficiencies, lower capital costs and a smaller overall footprint than what can be achieved by utilizing separate components for each required unit process/operation in conventional coal to hydrogen systems.

Specifically, this project developed a novel membrane reactor process that combined hydrogen sulfide removal, hydrogen separation, carbon dioxide separation and water-gas shift reaction into a single membrane configuration. The carbon monoxide conversion of the water-gas-shift reaction from the coal derived syngas stream is enhanced by the complementary use of two membranes within a single reactor to separate hydrogen and carbon dioxide. Consequently, hydrogen production efficiency is increased. The single membrane reactor configuration produces a pure H_2 product and a pure CO_2 permeate stream that is ready for sequestration. This project focused on developing a new class of CO_2-selective membranes for this new process concept.

Several approaches to make CO_2-selective membranes for high-temperature applications have been tested. Membrane disks using the technique of powder pressing and high temperature sintering were successfully fabricated. The powders were either metal oxide or metal carbonate materials. Experiments on CO_2 permeation testing were also performed in the temperature range of 790 ° to 940 °C for the metal carbonate membrane disks. However, no CO_2 permeation rate could be measured, probably due to very slow CO_2 diffusion in the solid state carbonates.

To improve the permeation of CO_2, one approach is to fabricate membranes with liquid or molten carbonates. Several different types of dual-phase membranes were fabricated and tested for their CO_2 permeation in reducing conditions without the presence of oxygen. Although the flux was quite low, on the order of 0.01 to 0.001 cc STP/cm^2/min, the selectivity of CO_2/He was almost infinite at temperatures of about 800°C.

A different type of dual-phase membrane prepared by Arizona State University (ASU) was also tested at GTI for CO_2 permeation. The measured CO_2 fluxes were 0.015 and 0.02 cc STP/cm^2/min at 750 ° and 830 °C, respectively. These fluxes were higher than the previous flux obtained (~0.01 cc STP/cm^2/min) using the dual-phase membranes prepared by GTI. Further development in membrane development should be conducted to improve the CO_2 flux.

ASU has also focused on high-temperature permeation/separation experiments to confirm the carbon dioxide separation capabilities of the dual-phase membranes with $La_{0.6}Sr_{0.4}Co_{0.8}Fe_{0.2}O_{3-\delta}$ (LSCF6482) supports infiltrated with a Li/Na/K molten carbonate mixture (42.5/32.5/25.0 mole %). The permeation experiments indicate that the addition of O_2 does improve the permeance of CO_2 through the membrane.

A simplified membrane reactor model was developed to evaluate the performance of the process. However, the simplified model did not allow the estimation of membrane transport area, an

important parameter for evaluating the feasibility of the proposed membrane reactor technology. As a result, an improved model was developed. Results of the improved membrane reactor model show that the membrane shift reaction process has promise as a means to simplify the production of a clean stream of hydrogen and a clean stream of carbon dioxide. The focus of additional development work should address the large area required for the CO_2 membrane as identified in the modeling calculations.

Also, a more detailed process flow diagram should be developed that includes integration of cooling and preheating feed streams as well as particulate removal so that steam and power generation can be optimized.

For the tubular membranes that were fabricated by solution impregnation with metal carbonates, difficulties were encountered in removing impurity salts that were trapped inside the porous support tube. The membrane tube would continue losing weight even after heating to 500 °C in air and could not maintain its nonporous characteristics. This approach was therefore abandoned.

Dual-phase membranes with molten carbonates were subsequently shown to have CO_2 permeability in reducing conditions without the presence of oxygen; they were also tested for H_2S permeation. Permeation tests were conducted with a gas feed composition consisting of 33.6% CO_2, 8.4% He, 57.6% H_2 and 0.4% H_2S at temperatures between 820° and 850 °C and a pressure of 1 bar. On the permeate side, hydrogen was used as a sweep gas to react with any sulfide ion that permeated through the membrane to form H_2S. The measured H_2S flux was on the order of 0.01 to 0.03 cc STP/cm^2/min. The flux of H_2S was considerably higher than that of CO_2, with a H_2S/CO_2 selectivity approaching 2000. This type of membrane can be used for front-end sulfur removal in the single membrane reactor configuration.

In the area of hydrogen transport membranes, the palladium-copper (Pd-Cu) alloy membrane was selected over the proton-conducting ceramic membrane for hydrogen separation section of the single membrane reactor configuration. However, the metallic membrane should be evaluated for its thermal stability in the temperature range of interest in this project, 750 °to 900 °C. The other issue is sulfur tolerance of the metallic membrane. In general, high temperature operation should be more favorable for sulfur resistance. Hydrogen permeation of a commercial Pd-Cu alloy foil was tested at 850 °C for continuous operation of about 2 weeks. There was no performance degradation observed in terms of hydrogen flux, which is a good indication of its thermal stability at this high temperature. A permeation test was also performed with a feed gas containing 1000 ppm H_2S, 50% H_2 and balance He at 850 °C. After 8 hours operation no hydrogen flux decline was observed, indicating good sulfur resistance for this material.

INTRODUCTION AND BACKGROUND

The objective of this project was to develop a novel complementary membrane reactor process that can consolidate two or more downstream unit operations of a coal gasification system in a single module for production of a pure stream of hydrogen and a pure stream of carbon dioxide. The overall goals were to achieve higher hydrogen production efficiency, lower capital costs and a smaller overall footprint than what could be achieved by utilizing separate components for each required unit process/operation in conventional coal-to-hydrogen systems. Since the process would remove H_2S, it is particularly suitable for the high-sulfur Illinois coals.

Specifically, this project was to develop a novel membrane reactor process that combines hydrogen sulfide removal, water-gas shift reaction, hydrogen separation and carbon dioxide separation in a single membrane configuration. The CO conversion of the water-gas-shift reaction from the coal-derived syngas stream is enhanced by the complementary use of two membranes within a single reactor to separate hydrogen and carbon dioxide. Consequently, hydrogen production efficiency is increased. The single membrane reactor configuration produces a pure H_2 product and a pure CO_2 permeate stream that is ready for sequestration.

In this project, Gas Technology Institute and Arizona State University developed a new class of nonporous membranes for H_2S removal and CO_2 separation. The hydrogen-transport metallic membrane or mixed proton-electron conducting perovskite membrane can be used for hydrogen separation. Both of these nonporous membranes would have 100% selectivity to CO_2 and H_2 respectively. Bulk removal of hydrogen sulfide can be achieved with the use of a material similar to the CO_2-selective membranes. These membrane materials are operating at the same temperature and pressure and therefore can be fabricated into a single reactor module.

Gasification is a promising technology for the production of hydrogen from coal. Gasification combines coal, steam and oxygen to produce synthesis gas, mainly hydrogen and carbon monoxide. After being cleaned of impurities such as sulfur, the synthesis gas is shifted using the water-gas shift reaction, (Reaction 1), to generate additional hydrogen and convert carbon monoxide to carbon dioxide. Hydrogen is subsequently separated from the gas stream, typically using Pressure Swing Adsorption (PSA) technology. If necessary, CO_2 can be removed prior to the PSA unit to obtain a CO_2-enriched stream and increase the hydrogen recovery in the PSA unit. A simplified flow diagram for this conventional process is shown in Figure 1.

$CO + H_2O = CO_2 + H_2$ + 41 KJ/mole water-gas-shift reaction Reaction 1

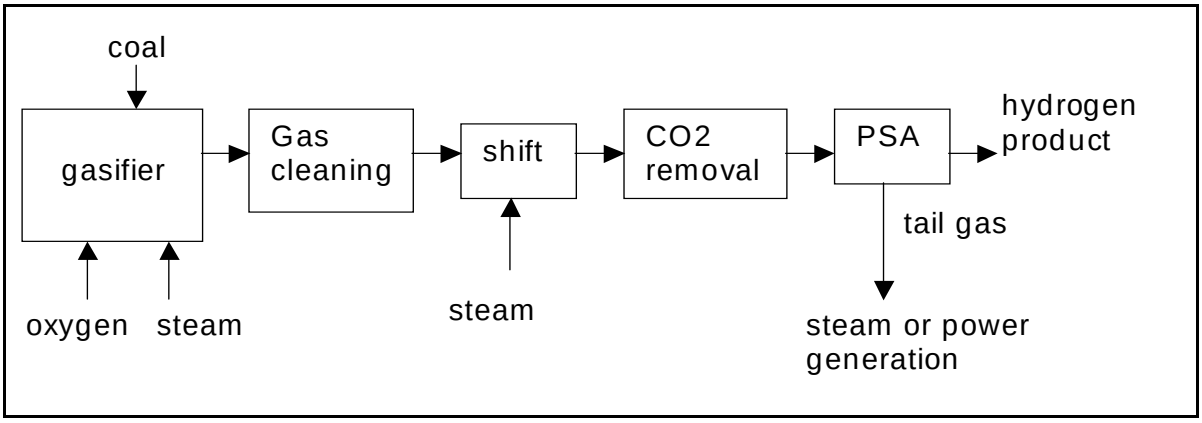

Figure 1. Conventional Hydrogen Production from Coal Gasification Process

The concept envisioned by GTI consolidates the major downstream units of a gasification system into a single reactor configuration. The concept employs gas permeation membranes to separate H_2S, CO_2, and H_2 individually, combined with the water-gas-shift reaction within a single membrane module. The three membranes are arranged in such a way that the feed or the retentate (the nonpermeate) stream flows through the three membranes in series while the individual permeates, H_2S, CO_2, and H_2 are obtained separately. Because the three membranes can be operated at about the same temperature and pressure, they can be housed in a single pressure vessel to reduce the footprint and simplify operation.

The first membrane preferentially allows H_2S to permeate through; the second membrane is selective to CO_2; and the third is a hydrogen-selective membrane. Figure 2 shows the proposed membrane configuration. The removal of both H_2 and CO_2 by the complementary use of the two membranes within a single reactor also drives the water-gas-shift reaction beyond its equilibrium limit in the absence of product removal via the membranes. Figure 3 is a simplified flow diagram showing the hydrogen production process from coal gasification using the proposed complementary membrane reactor configuration. All four major downstream units in Figure 1 have been combined into "one box" in Figure 3. The syngas exiting the proposed complementary membrane reactor, which is significantly reduced in its volume after removal of CO_2 and H_2, can be recovered for its heat and any residual fuel content for steam or power generation. Additional gas conditioning, if necessary, may be employed to remove other trace contaminants such as nitrogen, halogens, or metal compounds from the non permeate gas with much smaller equipment due to the reduced molar flow.

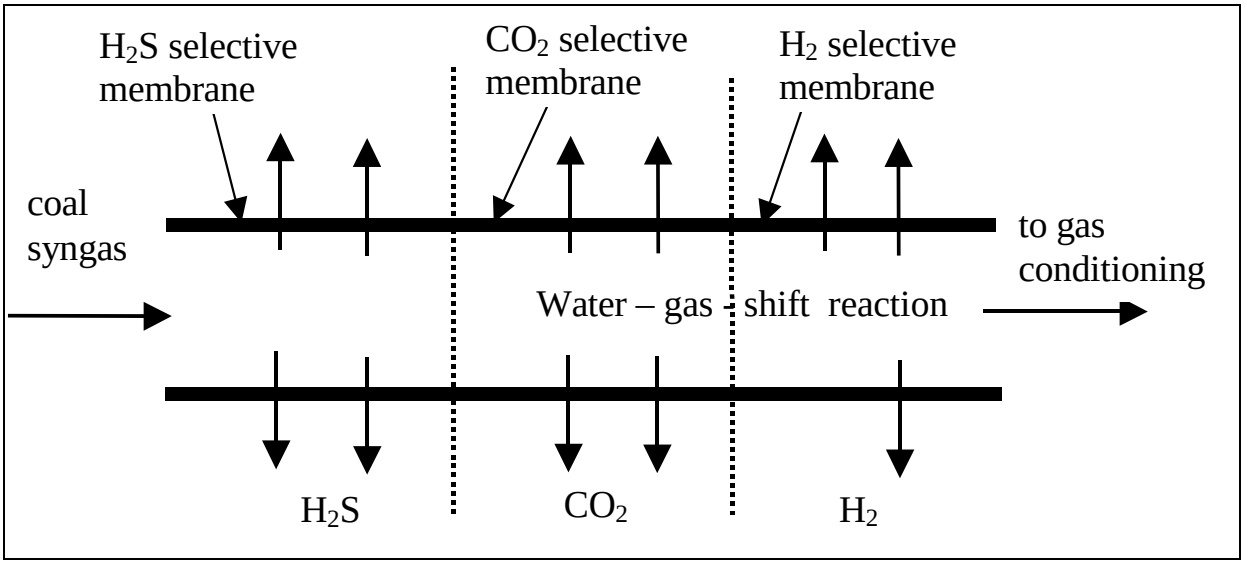

Figure 2. Complementary Membrane Reactor Configuration for CO_2 and H_2 Separation with H_2S Removal

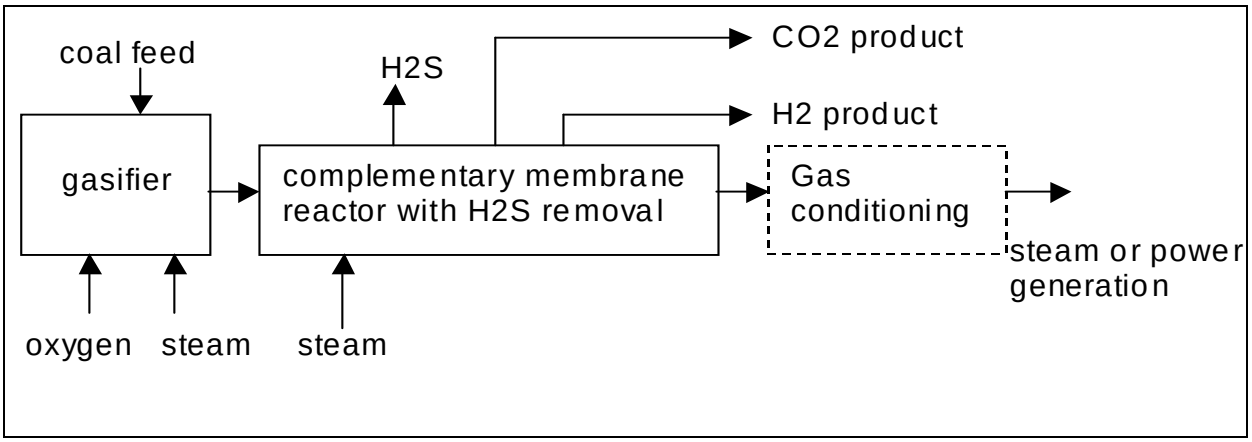

Figure 3. Hydrogen Production from Gasification System Using the Complementary Membrane Reactor Configuration

The ideal membrane materials for the proposed concept are dense and non-porous with near 100% selectivity to H_2S, CO_2 or H_2 respectively. For the temperature ranges between 600 and 1000 ^oC, a new class of calcium-based metal oxide membranes is suggested as candidate materials for H_2S removal. Similar calcium-based metal carbonate or oxide membranes are ideal for CO_2 separation. Mixed protonic-electronic conducting membranes such as perovskite or pyrochlore ceramic materials are known to have infinite selectivity to hydrogen between 600 and 1000 ^oC and are well suited for the third stage of the proposed process. The selection of these types of membrane materials for the "one box" single membrane reactor configuration results in a pure CO_2 product and a pure H_2 product without the need of any further purification of those component streams.

Work on developing nonporous CO_2-selective membranes was conducted at ASU laboratories. One approach was to use pressing and sintering techniques from metal oxide or metal carbonate powders to fabricate dense membranes. Another approach was to impregnate metal carbonate particles onto a porous support. Several metal carbonate disks were fabricated and tested for their CO_2 permeation. For the impregnation method, thermal stability of the fabricated tubular membranes was investigated by attempting to remove solid impurities from the membrane tubes.

CO_2 diffusion in the solid state metal carbonates was expected to be very slow. To improve the permeation of CO_2, membranes with liquid or molten carbonates were fabricated. These dual-phase membranes were tested for their CO_2 permeation in reducing conditions without the presence of oxygen. Encouraging preliminary results were obtained.

The project team also evaluated membrane materials for the hydrogen separation section of the single membrane reactor configuration. Palladium-copper alloy membranes were selected over proton-conducting ceramic membranes as the candidate hydrogen-selective membrane. The current state-of-the-art proton conducting ceramic membranes still fail to demonstrate good flux and chemical stability with CO_2 and/or H_2S. However, the metallic membrane should be evaluated for its thermal stability in the temperature range of interest in this project, 750 ° - 900 °C. The other issue is sulfur tolerance of the metallic membrane. Results for both thermal stability and sulfur tolerance are discussed in this report.

Encouraging preliminary results were obtained for CO_2 permeation using dual-phase membranes incorporating molten carbonates in porous stainless steel disks. Molten carbonate membranes are also known to exhibit transport property for sulfide ion species under the electrical potential driving force.[1] Removal of H_2S from a fuel gas stream by electrochemical membrane separation has been reported in the literature. [2,3,4,5] With the addition of an electronic conducting phase to the membrane structure, the membrane can potentially remove H_2S simply under the partial pressure difference of H_2S between the feed side and the permeate side of the membrane. Figure 4 shows the transport mechanism for the mixed ionic-electronic conducting membrane for H_2S removal.

On the permeate side of the membrane, the transported sulfide ions combine to form elemental sulfur, which could be carried away by an inert sweep gas and be condensed downstream of the membrane unit. On the feed side, H_2 could be produced by the dissociation of H_2S. In the presence of a large concentration of CO_2, the following side reactions can take place and compete with the transport of the sulfide ion:

Feed side: $2\ CO_2 + 2\ e^- \rightarrow CO + CO_3^{2-}$

Permeate side: $CO_3^{2-} \rightarrow CO_2 + ½\ O_2 + 2\ e^-$

Consequently, CO_2 permeation instead of the intended transport of sulfide may occurHowever,the generation of the CO_3^{2-} ion is thermodynamically less favorable than S^{2-} generation from H_2S dissociation.

In comparison with the electrochemical membrane, the dual-phase membrane not only offers the advantage of no need to supply an external electrical current, it also eliminates the need for electrodes. The sulfur compatibility issue for the electrode materials, especially the cathode, is a major hurdle for the electrochemical membrane system. [5] The sulfide-ion-conducting membrane can also directly produce elemental sulfur downstream of the membrane, which can eliminate the Claus plant that is typically needed in other sulfur removal technologies.

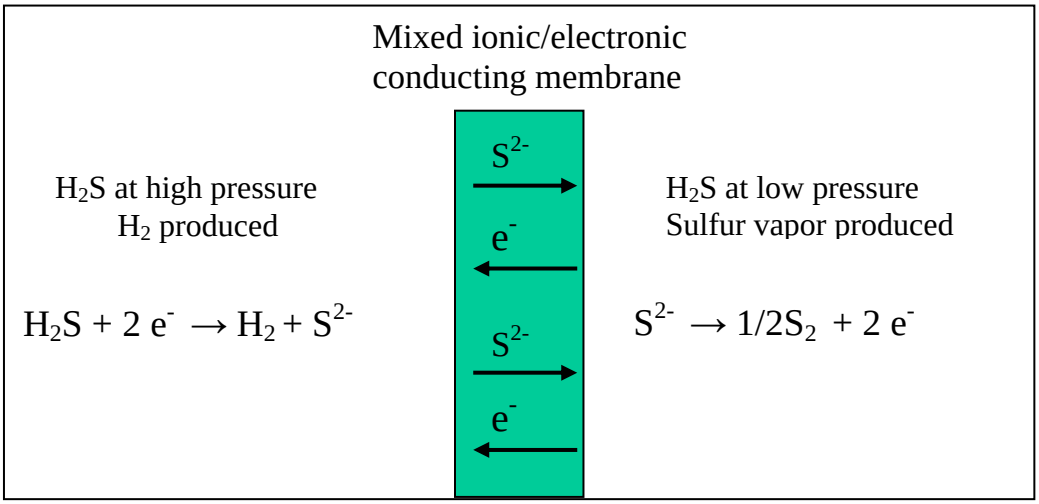

Figure 4. Transport Mechanism for H_2S Separation Using Mixed Ionic/Electronic Conducting Membrane

The concept of using the dual-phase membrane for H_2S separation was tested at GTI's laboratory. Additionally, a different type of dual-phase membrane prepared by Arizona State University was also tested at GTI for CO_2 permeation. The previous results obtained by the ASU team indicated that practically no CO_2 permeated the membrane when CO_2 was the only component present on the feed side. Almost immediately after O_2 was introduced with CO_2 to the upstream side, permeance of CO_2 increased dramatically. Permeation tests were conducted at GTI to verify these results.

ASU conducted high temperature permeation/separation experiments to confirm the CO_2 separation capabilities of the dual-phase membranes. In addition, GTI used a modeling approach to examine the proposed single membrane reactor process in comparison with the conventional H_2-selective or CO_2-selective membrane reactor process. Analysis of the process with a commercial flow sheet simulator, HYSYS, was used to calculate the expected performance. Although H_2S can be removed using the same type of dual-phase membranes as the CO_2-selective membrane, H_2S removal was not considered in the modeling work.

EXPERIMENTAL

The project team synthesized batches of the nanosized $CaCO_3$ and CaO powders, analyzed the powders for chemical and physical characteristics, fabricated the membranes, tested them in a permeation unit, and demonstrated the feasibility of CO_2 separation and H_2S removal using the high temperature Ca-based membranes. Perovskite-type ceramic membranes were tested for their chemical stability under H_2S and CO_2 environments. Theoretical models for CO_2 permeation through the Ca-based membranes and H_2 permeation through the perovskite membranes were developed. Computer simulations were performed to evaluate the performance of H_2 production from coal gasification systems based on the complementary membrane water-gas-shift reaction process. The program of detailed experimental and theoretical work, consisted of the six tasks as detailed below.

Task 1.0 – Prepare and Test CaO Membrane Material

This task was performed at Arizona State University under the guidance of Dr. Jerry Lin.

Membrane synthesis and characterization: Commercially available CaO is not nanostructured. Thus, nanostructured CaO was prepared by the sol-gel method in the laboratory. CaO membrane disks were prepared by pressing powders of CaO and sintering the green body at an elevated temperature. The membrane disks were characterized by nitrogen adsorption porosimetry and helium permeation to examine the pore structure. CaO membranes were prepared with different crystal sizes, pressing pressures and sintering temperature and characterized for their gas-tightness (for dense membranes) and pore size (for porous membranes).

Carbon dioxide sorption equilibrium isotherms on CaO pellets were measured at p_{CO2} range of 0 to 1 bar at 700 ^{o} - 900 ^{o}C. The experiments were conducted on a Cahn micro-electronic balance system available in Dr. Lin's laboratory (ASU). Sorption uptake versus time curves were measured in the same temperature range on the CaO particles of different sizes. Surface reaction rate and diffusivity of carbon dioxide in the particle were calculated. Similar experiments were performed for the desorption rates. Disks of CaO were subjected to pressure swings of carbon dioxide at a high temperature (e.g., 800 ^{o}C). The mechanical integrity of the disks was examined. Observation of pulverization of the disks after this test would indicate the problem of CO_2 embrittlement due to structural change accompanied by variation of CO_2 loadings.

Permeation testing: CO_2 permeance can be readily predicted from the CO_2 adsorption equilibrium and diffusion properties. CO_2 permeation and separation tests on the CaO membrane disks were performed. Membranes were initially sealed with graphite seals. Single gas permeance was measured with pure CO_2 in the feed at 700^{o} to 900 C. Multiple gas separation was measured with equal molar CO_2-He mixture as the feed. Nitrogen was used as the sweep gas in the downstream line

Task 2.0 – Prepare and Characterize $CaCO_3$ Membrane Material

Nanoparticle synthesis and characterization: The primary aim of this task was to develop a CO_2 membrane based on nanosized $CaCO_3$ particles to increase the overall permeation rate of CO_2. The nanosized $CaCO_3$ particles were prepared by a slurry-carbonation technique. A supersaturated $Ca(OH)_2$ slurry was prepared in water. Next, CO_2 gas was bubbled through the slurry to generate CO_3^{2-} ions in solution, which would react with Ca^{2+} ions from $Ca(OH)_2$ to precipitate $CaCO_3$ particles. Anionic or cationic surfactants were also added to the slurry in small concentrations (< 1 wt %) to study their effect on the $CaCO_3$ particle size. The slurry was filtered and dried in a vacuum oven at 50 °C to recover $CaCO_3$ solids. The synthesized particles were next characterized in detail for their particle size (laser particle size analyzer), chemical structure (XRD, SEM), and pore-structural characteristics (low-temperature N_2-adsorption methods, such as BET).

Membrane fabrication: In this task, a supported nonporous $CaCO_3$ membrane was prepared by *in-situ* precipitation technique. A porous alumina tube with about 50 nm pore size was used as a support for the membrane. The tube was closed at one end and filled with a CO_3^{2-} ion solution (e.g., Na_2CO_3). It was immediately dipped in another solution containing Ca^{2+} ions [e.g., $Ca(NO_3)_2$]. The particles of $CaCO_3$ were allowed to grow at the interface and fill the pores in the alumina support. Concentration, pH, temperature, and precipitation time were carefully monitored to prepare membranes with the desired characteristics. The $CaCO_3$ membranes thus prepared were analyzed to verify the nonporous surface and dense coverage. Scanning Electron Microscopy (SEM) was used primarily to study the morphology and thickness of the $CaCO_3$ membranes. Several $CaCO_3$ membranes, with nonporous and thin-layer coverage, were selected for permeation testing.

Task 3.0 – Construct a New Permeation Unit

A new membrane permeation unit was constructed with the capability of handling H_2S-containing gas streams. The unit was operated at a pressure up to 10 atm. The membrane module was designed to measure permeation flux for membranes in either tubular or disk form. For tubular membranes, pure component gas or mixtures from the gas feeding system flows into the shell side of the membrane tube and the permeate gas is collected on the tube side of the membrane for flow measurement and gas analysis. An inert gas was used as sweep gas for the permeate. The membrane was housed in an existing high-temperature tubular furnace equipped with all the necessary instrumentation including a gas chromatograph (GC) to measure CO_2 concentration in the permeate stream. The unit was constructed from existing GTI equipment with the addition of instrumentation and a permeation cell.

Task 4.0 – Test Ca-Based Membranes in the New Permeation Unit

The $CaCO_3$ membranes selected in Task 2 were tested for CO_2 permeabilities and separation factors in the permeation unit built under Task 3. Pure CO_2 and CO_2/He gas mixture was used as the feed stream to measure CO_2 flux and any He crossover through leakage. The permeation results from the nonporous $CaCO_3$ membrane tests compared with those from microporous CaO membranes of Task 1.

The CaO membranes prepared at ASU in Task 1 were sent to GTI for permeation measurement of H_2S in the new permeation unit. The H_2S compositions in the feed stream were prepared according to the typical syngas compositions from the gasification of a high-sulfur coal such as Illinois No. 6. The CaO membranes were also pre-sulfided to form a nonporous CaS layer to increase H_2S selectivity before permeation testing. Gas mixtures of CO_2/H_2S were also tested for their separation factors. The permeation testing was studied at various temperatures between 700° and 900°C.

Task 5.0 – Prepare and Test Proton-Conducting Membranes

The objective of this task was to evaluate the feasibility of using proton-conducting membranes for H_2 separation in the proposed "one box" membrane scheme. The candidate membrane materials were selected based on recommendations from prior work or on-going research conducted at GTI. These included doped perovskites and the pyrochlore materials. Membrane materials were prepared in disk form by uniaxial pressing to a diameter of about 1 to 3 cm. A special high-temperature sealing technique developed at GTI was applied to seal the ceramic membranes and the test fixture. Feed gases consisting of H_2, CO_2 and up to 200 ppm of H_2S were tested for H_2 flux as well as their chemical stability. Tests were conducted in the same temperature range as in Task 4, i.e. 700º to 900ºC.

Task 6.0 – Modeling and Process Simulation

One objective of this task was to understand the transport mechanisms for both the Ca-based and the perovskite-type membranes. A permeation model based on traditional solution-diffusion mechanisms and non-equilibrium thermodynamics was formulated. Computer simulations were performed to reveal any important material properties that could affect gas permeation. Whenever possible, experimental data from the results of membrane material characterization in Task 1 and 2 were used in the model.

Another objective of this task was to evaluate the overall H_2 production performance from coal gasification systems based on the proposed complementary membrane water-gas-shift reaction process. A commercial simulation package, HYSYS, in conjunction with the membrane permeation models mentioned above was used for this task.

RESULTS AND DISCUSSIONS

Task 1.0 – Prepare and Test CaO Membrane Material

This task was performed at Arizona State University (ASU) under the guidance of Dr. Jerry Lin.

Metal oxide membrane (ASU)

One route to prepare an unsupported CO_2 membrane is by the pressing technique from metal oxide powders. One membrane disk sintered at 1000°C did not result in the desired gas-tightness after reaction with CO_2 at 900°C. In order to sinter the membrane at a higher temperature (1250°C), an yttria-stabilized zirconia (YSZ) plate was used instead of alumina plates, to avoid the undesired reactions between CaO and alumina at above 1000°C. Helium permeation at room temperature was conducted to check gas-tightness.

Dual-phase membrane (ASU, GTI)

In related research, much effort has been placed on the development of a stable, dual-phase membrane for CO_2 separation. In a recent publication (6), it was reported that a dual-phase membrane consisting of a stainless steel support infiltrated with molten carbonate is selective to CO_2 at high temperatures (400^o to 600^oC). However, O_2 is required for this dual-phase membrane. In the presence of CO_2, O_2, and electrons provided by the metallic support, CO_3^{2-} can be produced and transported through the molten carbonate. However, over time at high temperatures, the formation of iron oxides on the surface of the stainless steel supports renders the membranes ineffective. In this project, dual-phase membranes with an oxidation-resistant ceramic phase were fabricated by liquid infiltration of molten carbonates. The membranes were characterized by X-ray diffraction (XRD) as well as He permeation at room temperature. High temperature CO_2 permeation tests were also conducted.

CO_2 diffusion in the solid state metal carbonates was expected to be very low. To improve the permeation of CO_2, membranes with molten $CaCO_3$ were fabricated. Another powder was added to the $CaCO_3$ to form a eutectic mixture so that the melting point was lowered to below 700^oC. Porous stainless steel support disk was infiltrated with the molten carbonate by heating the powders and the disk together to a temperature of about 750 ^oC in CO_2 atmosphere. The use of CO_2 was to avoid calcination of the membrane at high temperatures. The stainless disk had a diameter of 2.22 cm (0.875 inch), a thickness of 0.16 cm (0.062 inch) and a pore size of 0.5 micrometer (μm). The fabricated membrane disks were first checked for He leakage at room temperature to ensure that the pores were completely filled with the carbonate salts. High temperature CO_2 permeation using glass-based sealant was then conducted. Tests were also conducted with stainless steel disks filled with other molten carbonate salts.

Task 2.0 – Prepare and Characterize CaCO3 Membrane Material

Supported tubular membrane (GTI)

In this approach, the membranes were prepared by depositing the desired metal carbonate powders onto a porous support tube. The tubular membrane would lose its weight after heat treatment at about 500°C in air. This could be due to the presence of impurity salts such as $CaCO_3$, $CaCl_2$, Na_2CO_3, NaCl, $Ca(OH)_2$, and NaOH including their hydrated forms that were left behind from the impregnating solution. It is necessary to remove these solids from the pores to synthesize a good-quality membrane, consisting primarily of $CaCO_3$. Simple rinsing with water was not enough to wash away the solids in the pores of the support tube. More studies were conducted to understand the nature of solids trapped within the pores of the tube. It appeared that the trapped solids needed a much longer time to dissolve and diffuse out into the water. A high-pressure water pump was used to force water through the pores to the other side of the tube. If the solid impurities would dissolve in the flowing water, they would come out of the pores as well.

The other method attempted to remove the solid impurities from the pores was by switching the cation solution from the inside of the tube to the outside. Earlier membrane tubes were prepared with $CaCl_2$ solution inside the tube, which made it difficult to wash away $CaCl_2$ left behind. A few membranes were synthesized with the $CaCl_2$ solution outside and the Na_2CO_3 solution inside. It was hoped that the Na_2CO_3 solution embedded in the inside wall of the tube would be easier to remove.

Metal carbonate disk membrane (GTI)

Instead of starting from CaO powder, a new approach to synthesize $CaCO_3$ membranes was initiated. $CaCO_3$ nanoparticles were synthesized by carbonation of $Ca(OH)_2$ slurry to precipitate $CaCO_3$. A membrane in the form of a disc was prepared by pelletizing synthesized $CaCO_3$ nanoparticles followed by sintering at high temperature in CO_2 atmosphere. In addition, fine $CaCO_3$ powder purchased from Alfa Aesar was used as the source of carbonate powder. The purchased powder had a finer particle size than the in-house precipitated carbonate powder. Sintering of the $CaCO_3$ pellets was conducted at 1000°C and 7.1 bar CO_2 pressure. The high pressure CO_2 was maintained to avoid calcination of the membrane at high temperatures. Several sintered $CaCO_3$ membrane disks were evaluated for He leakage at room temperature. The disk was held between two rubber O-rings using Swagelok compression fittings. Under 0.3 barg He pressure on the feed side, the leak of He to the permeate side could be measured. High temperature CO_2 permeation was also performed using compression sealing method with graphite ferrules and graphite O-rings.

Task 3.0 – Construct a New Permeation Unit

To evaluate CO_2 permeation for the membranes developed in this project, a new membrane permeation unit was designed and constructed at GTI. The unit is capable of measuring H_2 and CO_2 flux for membranes in disk or tubular form. A photo of this unit is shown in Figure 5. The membrane cells were designed and built to measure gas permeation for both disk and tubular membranes. Figure 6(a) shows the design for the disk membranein which the membrane to be tested is attached or cemented to a ceramic tube. A glass/ceramics-based sealant material is used to seal the membrane. A CO_2 (or He for leak checking) gas flowing through an inner tube is in contact with the membrane and exits the system as a non-permeate gas diverted by an outer tube. An inert sweep gas passing through another inner tube is used to sweep the permeate stream from the membrane. The permeate is then sent to a GC for analysis.

The other design is for the supported tubular membrane as shown in Figure 6(b). In this design, the two ends of the membrane tube are connected to nonporous alumina tubes with Teflon® fittings and the entire tube is enclosed within another alumina tube to make a shell-and-tube module. The gas that permeates or leaks through the membrane tube is collected on the shell side and sent to a flow meter or GC for analysis. For high-temperature permeation testing, the glass/ceramics sealant is used to connect the membrane tube and the nonporous alumina tube, instead of the Teflon® fittings. An existing small furnace was used to heat the disk membranes. For the tubular membranes, leak checking was only conducted at room temperature. If the tubular membranes passed the ambient temperature leak test, a high-temperature permeation test for CO_2 was conducted.

Figure 5. Photo of GTI's Gas Permeation Unit

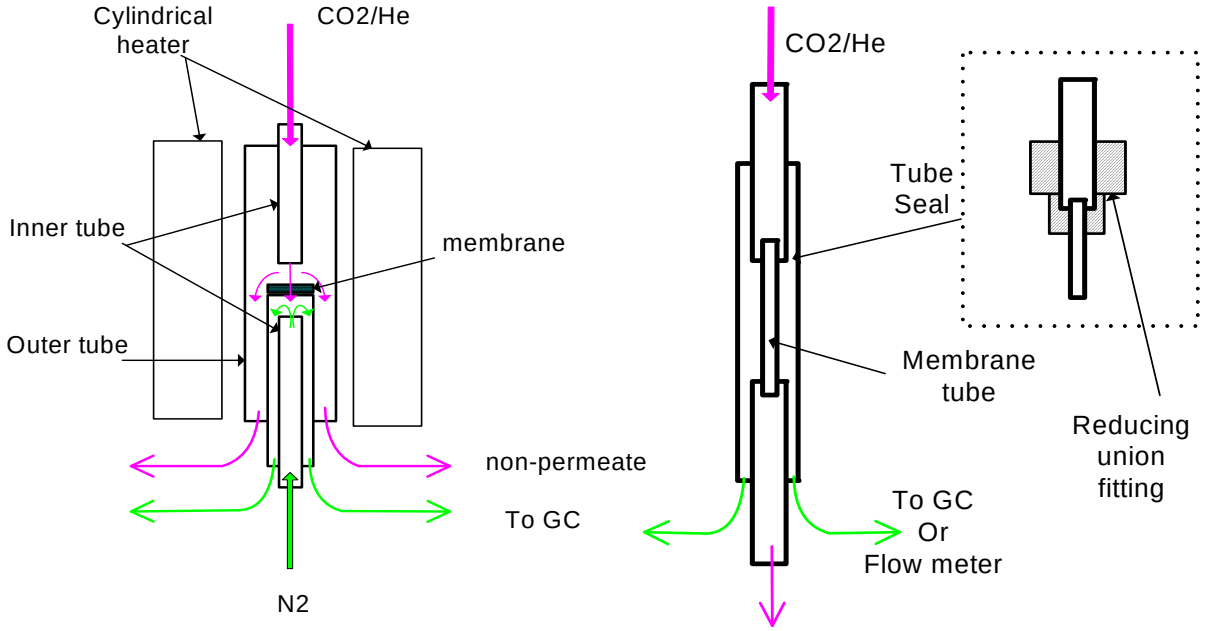

Figure 6. Two Membrane Cell Configurations: (a) Disk Membrane, (b) Tubular Membrane

Task 4.0 – Test Ca-Based Membranes in the New Permeation Unit

The CaO membrane sintered at 1250°C was tested for He permeation after treatment with CO_2 at 900°C. The results showed that the pretreatment characteristics of the CaO membrane sintered at 1000° and 1250°C were nearly identical. Interestingly enough, the CaO membrane sintered at the higher of the two temperatures showed very little change in He permeation characteristics after treatment with CO_2 at 900°C, as shown in Table 1.

Table 1. He Permeance for CaO Membranes Sintered at Different Temperatures Before and After High Temperature CO_2 Exposure

Sintering Temp (^oC)	Initial Permeance (moles/m^2·s·Pa)	Final Permeance (moles/m^2·s·Pa)
1000	7.81×10^{-6}	3.38×10^{-9}
1250	5.68×10^{-6}	3.59×10^{-6}

The table shows that the average He permeance of the CaO membranes sintered at the higher of the two temperatures is much too high to be effective. High temperature CO_2 exposure of the CaO membranes resulted in just 2.4% weight increase. The low increase in weight helps provide an idea of how little reaction there was between the CaO and CO_2 during the two-day period. In comparison, the CaO membrane sintered at the lower temperature experienced a decrease in He permeance from 7.81×10^{-6} to 3.38×10^{-9} moles/m^2·s·Pa after reaction with CO_2.

Supported tubular membrane (GTI)

The use of a high-pressure water pump did not produce satisfactory results in removing the impurities from the membrane tube. After forcing water for about 30 min, it was calculated that this process removed about 18 mg of solids out of the 23 mg present in the pores, leaving behind about 5 mg of solids trapped in the pores. When heated subsequently at 500°C in air, the membrane lost about 0.8 mg in mass. Since $CaCO_3$ does not decompose below 600°C, the weight loss was thought to be due to the presence of some other impurities. A helium leak check of the membrane tube also showed significant leakage.

Switching the cation solution from the inside of the tube to the outside also did not remove the solid impurities from the membrane tube effectively. After impregnation, repeated drying and rinsing resulted in a weight loss of the membrane tube, an indication of solid materials being removed. However, the membrane tube continued losing weight after being heated to 500°C in air, which could be due to decomposition of precursor solids left in the tube pores. The observed He leak for the membrane was also very high. This increase in the leak rate was the result of the heat treatment, which decomposed some of the solids in the tube.

These tests suggested that the solids left behind during the impregnation stage are difficult to remove by the procedures described above. Therefore, the tubular membrane approach was not continued.

Metal carbonate disk membrane (GTI)

For the metal carbonate membranes sintered from the in-house $CaCO_3$ powders, the density of the pellets was calculated to be approximately 2.4 g/cc, based on the weight and dimensions of the sintered pellets. The theoretical density of $CaCO_3$ is 2.71 g/cc. The calculated density of the pellets prepared from purchased $CaCO_3$ powder was about 2.52 g/cc, which was closer to the theoretical density of 2.71 g/cc. The increased dense structure of the disk from purchased powder may be due to its finer particle size.

At 0.34 barg (5 psig) He pressure on the feed side, the leakage of He to the permeate side of the membrane was approx. 0.07 cc/min or $1x10^{-9}$ moles/m^2·s·Pa, which is considered to be very good and demonstrated the dense structure of the membrane disk.

High-temperature sealing for the dense $CaCO_3$ membrane disk also presented a challenge. Several combinations of sealing materials were attempted to seal the $CaCO_3$ disks to the experimental setup. The materials included: pure glass, pure Duncan Glaze, 1:3 mixture of ceramic powder and glass, 1:4 and 1:9 mixtures of $CaCO_3$ powder and glass/Duncan Glaze, and cement mixed with Duncan Glaze. These sealing materials were applied to the disk followed by heating to temperature in the range of 880° to 970°C in 6.90 barg (100 psig) CO_2 pressure. However, none of these sealants were successful in sealing the membrane disk. It was discovered that the melt glass did not spread well on the surface of the $CaCO_3$ membrane disk, presumably due to poor surface adhesive force between the glass and the $CaCO_3$ materials.

The high-temperature sealing issue was eventually solved by employing a new permeation cell using a standard compression fitting of Swagelok type. Figure 7 shows the design of the permeation cell. The membrane disk and two O-rings were placed within a 1" x 1/2" stainless steel reducing union. The O-rings were then compressed by the tube connected to the reducing union (outer tube in Figure 7). The ferrules and the O-rings are made of graphite for high-temperature application, to 950°C in a non-oxidizing environment. Helium leakage rate across the O-rings or membrane was on the order of $1x10^{-8}$ moles/m^2·s·Pa, which is considered adequate for CO_2 permeation testing.

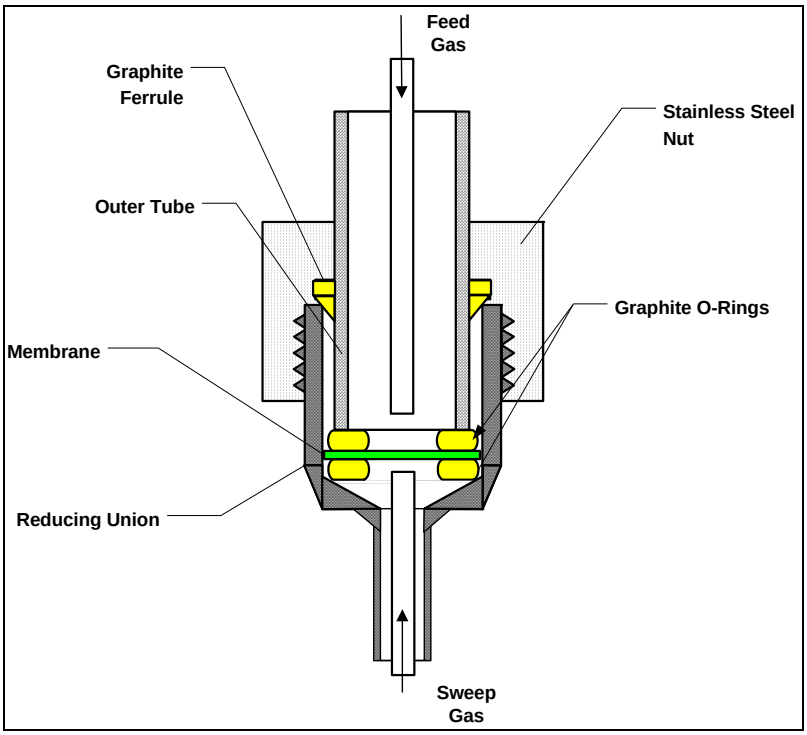

Figure 7. Schematic of Permeation Cell for Disk Membrane Using Graphite Ferrule and O-Rings

Permeation testing was conducted in the temperature range of 790° to 940°C with 75/25 CO_2/He in the feed and nitrogen as the sweep gas. The feed side pressure was maintained at 0.14 to 0.34 barg (2 to 5 psig) while the permeate side was about 0.14 barg (2 psig). The permeation experiment appeared to reach steady state very slowly with continued decreases of both CO_2 and He concentrations in the permeate side. Therefore, two overnight permeation experiments were conducted at 840° and 940°C. No CO_2 permeation rate could be measured because the concentration of CO_2 in the permeate was almost zero with only traces of He being detected. Another carbonate membrane was also tested for CO_2 permeation. Both CO_2 and He concentrations in the permeate were less than 0.1% each (balance N_2), with no CO_2/He selectivity. CO_2 and He probably leaked through the membrane following the Knudsen diffusion mechanism.

After the membrane disk was removed from the unit, the weight of the membrane was less than it was before the permeation testing. The membrane was further heated up to 900°C in an oven, and additional weight loss was observed. This indicated that the original dense carbonate membrane was partially decomposed to porous metal oxide structure, presumably in the permeate side. This was also consistent with the experimental observation that the CO_2 concentration in the permeate side tended to increase when the temperature was raised, perhaps due to calcination. The feed side probably still remained in a carbonated and dense form as it was in contact with CO_2 during the permeation experiment. The diffusion of CO_2 through the dense layer of $CaCO_3$ was probably very slow, which resulted in a nearly zero permeation of CO_2.

Dual-phase membrane (ASU, GTI)

For the dual-phase membrane, results of XRD analysis have shown that the doped ceramic and molten carbonate mixture do not react with each other at temperatures at or around 700^{o}C. Four-point method conductivity tests indicate that the ceramic phase has sufficiently high electronic conductivity for this purpose.

A lithium-base molten carbonate mixture was coated on the porous ceramic support by a liquid infiltration method. Helium permeances of the support before and after infiltration were on the order of 10^{-6} and 10^{-10} moles/m^2·Pa·s, respectively, indicating that the molten carbonate was able to sufficiently infiltrate the membrane and the final membrane was fairly gas-tight. Preliminary tests conducted previously showed very promising results using this membrane as a high-temperature separation media for CO_2. The membrane was sealed on a quartz tube with a commercial glass sealant. Separation tests were conducted at 750°C using either He or Ar as a sweep gas. The results indicated that essentially no CO_2 permeated the membrane when CO_2 was the only component present on the feed side. Almost immediately after O_2 was introduced with CO_2 to the upstream side, permeance of CO_2 increased dramatically to a flux of 48 cc/cm^2·min (57 kg/m^2·hr). However, the gas chromatograph (GC) indicated only very low values of O_2 on the permeate side of the membrane.

Because O_2 is not expected to be present in syngas derived from coal gasification systems, a stainless steel disk was used for infiltrating eutectic carbonate salts. About 0.27 g of carbonate salts were added to the porous disk. Helium leak check at room temperature confirmed that the pores of the membrane disk were completely blocked by the carbonate salts. The membrane disk was then impregnated with Ni by brushing with Ni/water slurry on both sides to give the membrane certain catalytic capability.

CO_2 permeation tests were conducted with 84/16 CO_2/He in the feed and N_2 in the permeate side as a sweep gas. The pressures were about 0.62 barg (9 psig) for both sides of the membrane. The membrane cell was first heated to about 920°C to melt the glass sealant and then decreased to 775°C for CO_2 permeation testing. Almost no Hecould be measured in the permeate side, indicating a very good seal as well as the nonporous characteristics of the membrane. After about 16 hours of CO_2 exposure on the feed side, no CO_2 was detected on the permeate side. When the temperature was increased to 800°C, CO_2 could be detected in the permeate side with its flux calculated as shown in Figure 8. Although the CO_2 flux was quite low, the almost infinite selectivity of CO_2/He was very encouraging.

Continuing to raise the temperature to 850°C, unfortunately, resulted in a huge leakage across the membrane. A possible reason for this could be due to calcination of carbonates, especially $CaCO_3$ or membrane failure.

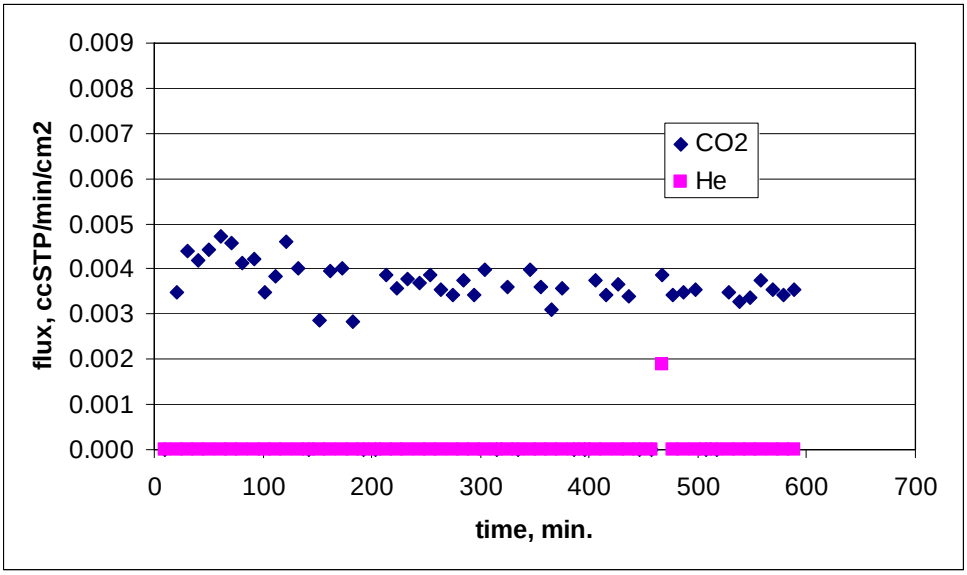

Figure 8. Permeation of CO_2/He (84/16 mole percent) Mixture in a Dual-Phase Membrane at 800°C and 1.61 barg (9 psig)

Tests were also conducted for a second type of carbonate salts with the same type of stainless steel disk. CO_2 permeation tests were conducted with 93/7 CO_2/He in the feed and nitrogen in the permeate side as a sweep gas. The pressures were about 3.45 barg (50 psig) on both sides of the membrane. The measured CO_2 fluxes are shown in Figure 9 at a temperature of 811°C. Again, no He could be observed in the permeate side. The CO_2 flux is higher than in Figure 8 perhaps due to higher partial pressure of CO_2 in the feed.

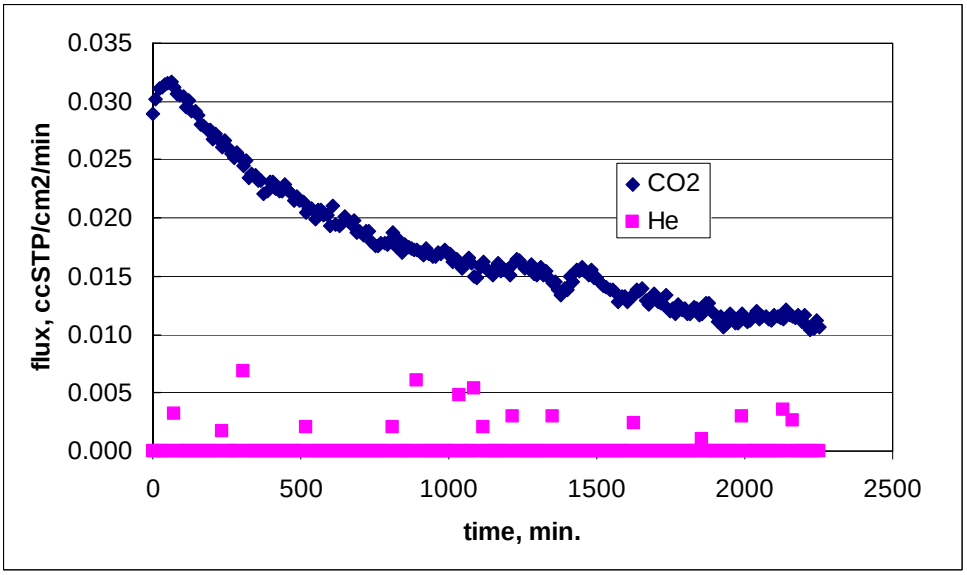

Figure 9. Permeation of CO_2/He (93/7 mole percent) Mixture in a Dual-Phase Membrane at 811°C and 3.45 barg (50 psig)

Testing of hydrogen transport membrane (GTI)

The long-term testing results of a $Pd_{80}Cu_{20}$ membrane is shown in Figure 4 for a 1-mm thick membrane at 850°C and 1 bar with 100% hydrogen in the feed side and N_2 in the permeate side. The membrane did not show any deactivation over a 12-day period. Figure 10 shows that Pd-Cu alloy membranes look promising for H_2 separation applications at temperatures greater than 800°C. Of course, for future commercial applications, much longer testing with real syngas will be required.

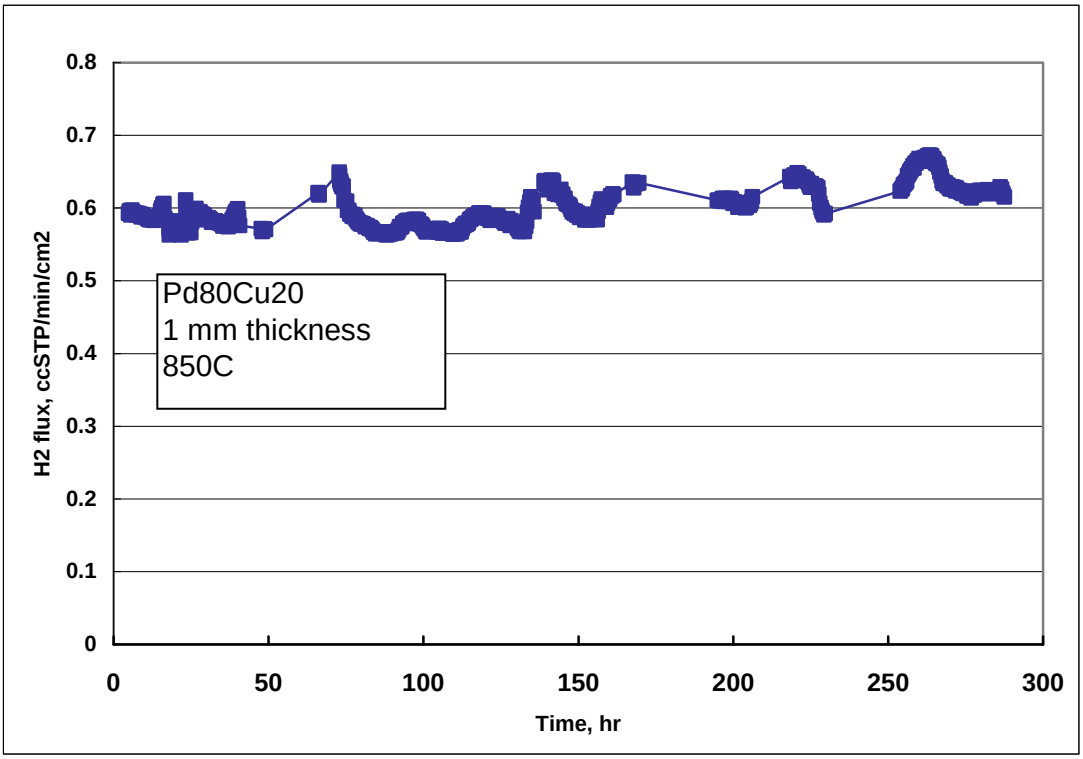

Figure 10. Hydrogen Permeation for Pd-Cu Alloy Membrane

Hydrogen permeation tests for the Pd-Cu membrane were also conducted with a 50/50 H_2/He feed containing 1,000 ppm H_2S at ambient pressure. Figure 11 shows the H_2 flux before and after the introduction of 1,000 ppm H_2S for a $Pd_{80}Cu_{20}$ membrane 1 mm thick at 850°C. As can be seen, there was no effect on the H_2 permeation after the membrane had been exposed to H_2S for about eight hours. Although coal-derived syngas can contain H_2S well above 1,000 ppm, especially for high-sulfur coal, using 1,000 ppm for the current tests is based on the assumption that a front end H_2S-selective membrane can remove the bulk of H_2S.

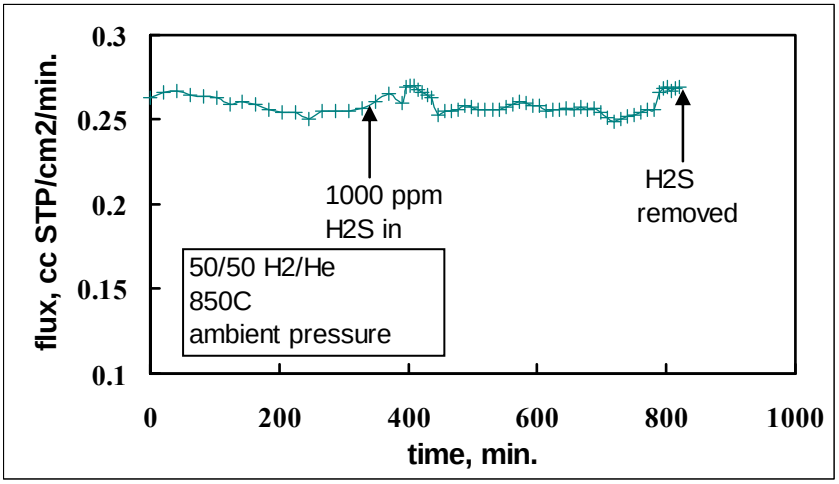

Figure 11. Effect of H_2S on Pd-Cu Alloy Membrane

H_2S permeation testing

Three membrane samples were successfully tested in the high temperature permeation unit. The first sample showed a stable H_2S flux of about 3 $x10^{-3}$ ccSTP/min/cm^2 at 824°C and 15 psig after 5 hours of operation. The flux of CO_2 was about 5.5$x10^{-2}$ ccSTP/min/cm^2. Helium was not detected in the permeate side indicating a good seal of the membrane. After raising the temperature to 850°C, the H_2S flux increased to about 4.7 $x10^{-3}$ ccSTP/min/cm^2 while CO_2 flux decreased to about 1.8 $x10^{-3}$ ccSTP/min/cm^2. This encouraging initial result prompted additional tests for two more membrane samples.

The second membrane was tested at 830°C and 1.03 barg (15 psig). The results are shown in Figure 12. The flux of H_2S actually was higher than that of CO_2. The calculated selectivity of H_2S/CO_2 was greater than 160. The selectivity of H_2S/CO_2 was defined as H_2S/CO_2 concentration ratio in the permeate side divided by H_2S/CO_2 concentration ratio in the feed side.

The temperature was then raised to 850°C and the results are shown in Figure 13 over a period of about 50 hours. Both H_2S and CO_2 fluxes continued increasing while no He was detected in the permeate side. The flux of H_2S was considerably higher than CO_2, with a H_2S/CO_2 selectivity approaching 1,000.

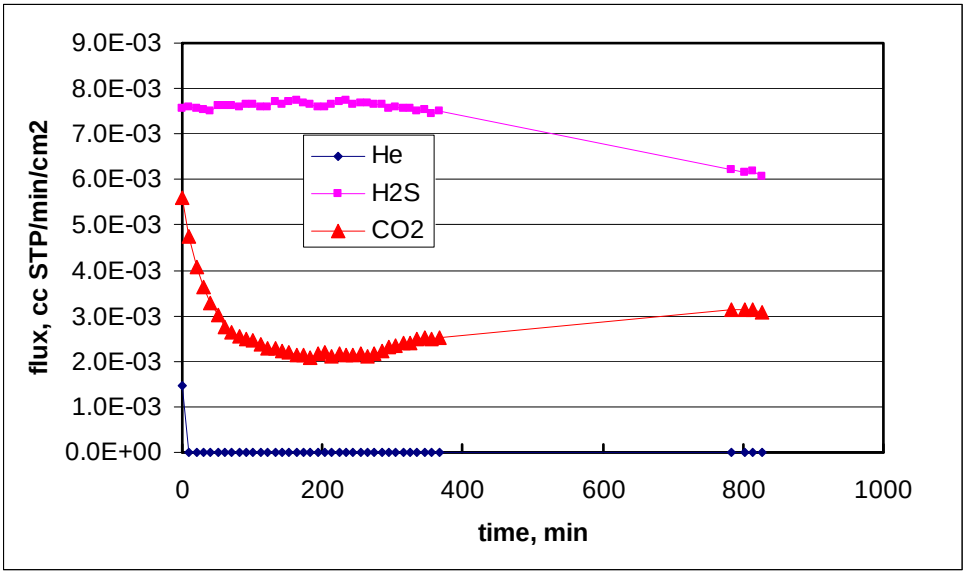

Figure 12. Permeation of CO_2, H_2S and He from a Gas Mixture for the 2nd Dual-Phase membrane at 830°C and 1.03 barg (15 psig)

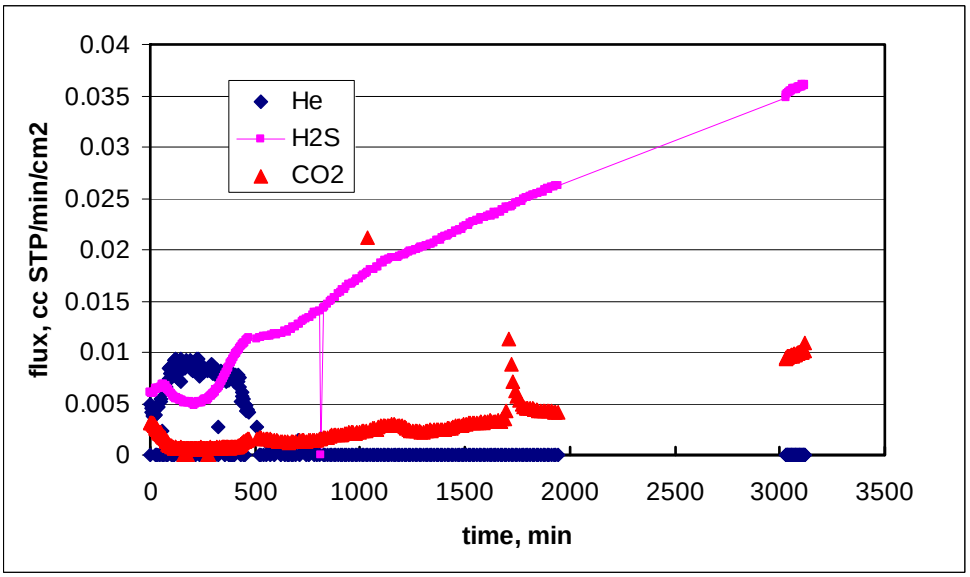

Figure 13. Permeation of CO_2, H_2S and He from a Gas Mixture for the 2nd Dual-Phase Membrane at 850°C and 1.03 barg (15 psig)

To further confirm the results, a third membrane disk was tested at 850°C over a period of about 40 hours as shown in Figure 14. Surprisingly, the CO_2 flux dropped to near zero while the flux of H_2S remained high. The selectivity of H_2S/CO_2 was close to 2000. Although He was detected in the permeate side, the average flux of He was about 1.86 x 10^{-3} ccSTP/min/cm^2, which

corresponds to a H_2S/He selectivity of 39. Due to scattering of the observed He fluxes and the absence of CO_2 in the permeate side, the membrane could be still considered leak tight.

This type of membrane can be used for the front end sulfur removal in the single membrane reactor configuration. The high selectivity of H_2S/CO_2, as observed from the above test results, is encouraging as only a minimum amount of CO_2 would be lost in the sulfur removal section of the single membrane reactor configuration.

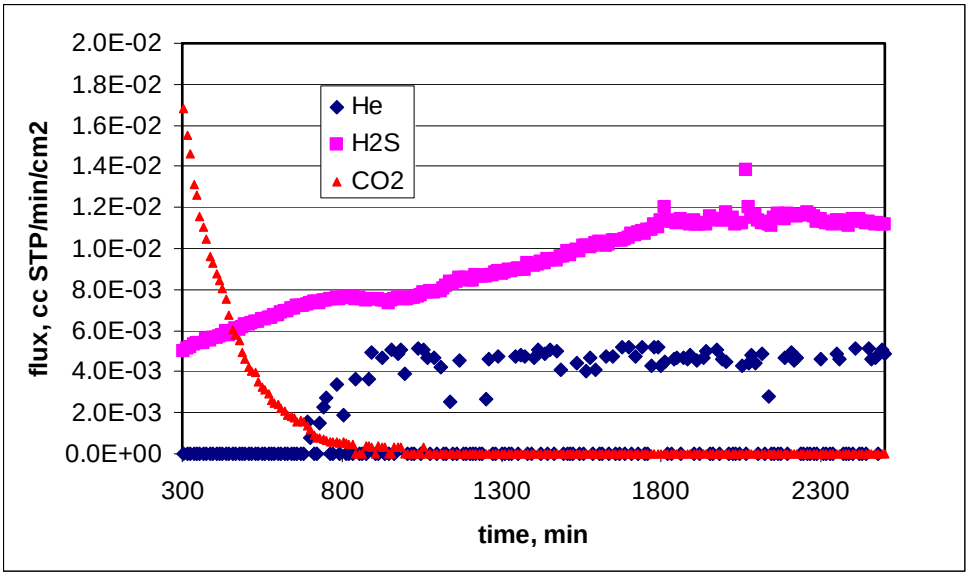

Figure 14. Permeation of CO_2, H_2S and He from a Gas Mixture for the 3rd Dual-Phase Membrane at 850C and 1.03 barg (15 psig)

CO_2 permeation testing

Several CO_2-selective dual-phase membranes prepared by Arizona State University were sent to GTI and tested in the high-temperature permeation unit. Figure 15 shows the fluxes of CO_2 and He at 752°C and 0.34 barg (5 psig) with a feed gas composition of 78.2% CO_2 and 21.8% He. Although the helium leak rate could be observed, the CO_2 flux was still higher than He and the selectivity of CO_2/He was higher than that calculated based on Knudsen diffusion. The measured CO_2 flux could be mainly attributed to the migration of CO_3^{2-} ion in the molten carbonate phase of the dense membrane.

The permeation testing continued with O_2 replacing helium in the feed side. The measured CO_2 and O_2 fluxes are shown in Figure 16 with a feed gas composition of 50.8% CO_2 and 49.2% O_2. In comparison with Figure 15, the CO_2 flux increased by about 4 times. The presence of O_2 in the feed probably promotes the formation of CO_3^{2-} ion:

Feed side: $CO_2 + 1/2\ O_2 + 2\ e^- \rightarrow CO_3^{2-}$

The O_2 flux was also measured in Figure 16. Although the O_2 flux was not exactly half of the CO_2 flux as required by the reaction stoichiometry, it was lower than the CO_2 flux.

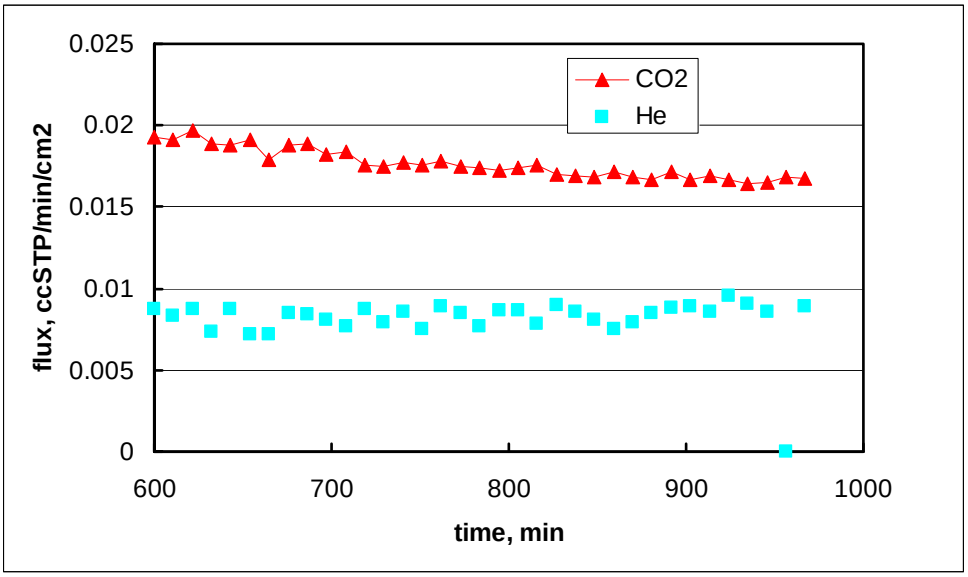

Figure 15. CO_2 Permeation for the Dual-Phase Membrane Prepared by ASU with 78.2% CO_2 and 21.8% He in Feed at 752°C

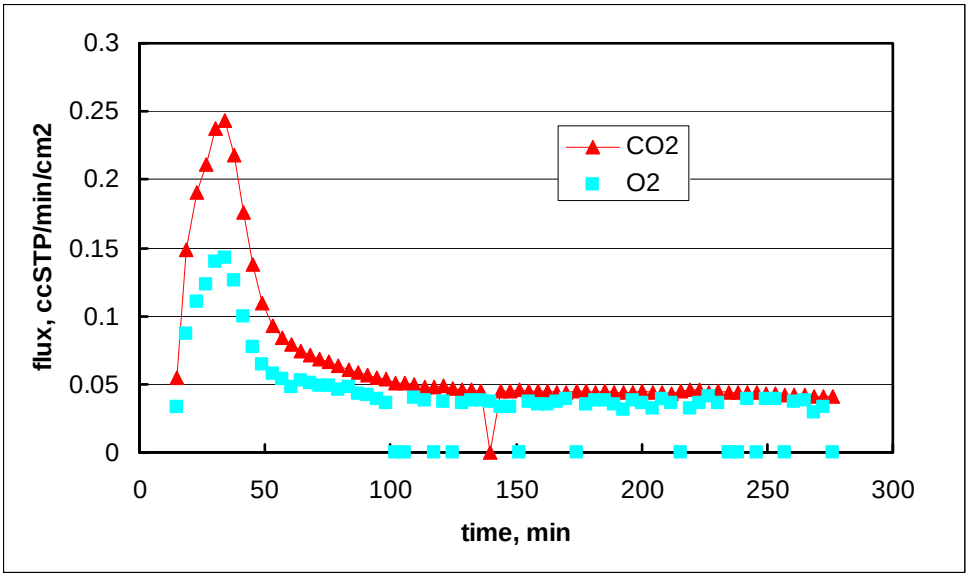

Figure 16. CO_2 Permeation for the Dual-Phase Membrane Prepared by ASU with 50.8% CO_2 and 49.2% O_2 in Feed at 752°C

Because of the small He leak rate detected for the permeation testing at 752ºC, the unit was heated to about 900ºC in an attempt to improve the sealing. The measured He leak rate indeed decreased. The membrane temperature was then reduced to 829ºC for further CO_2 permeation testing. The results are shown in Figure 17 with a feed gas composition of 78.2% CO_2 and 21.8% He at 0.34 barg (5 psig). In addition to the near zero flux observed for the He flux, the CO_2 flux was higher than that measured at 752ºC, as expected.

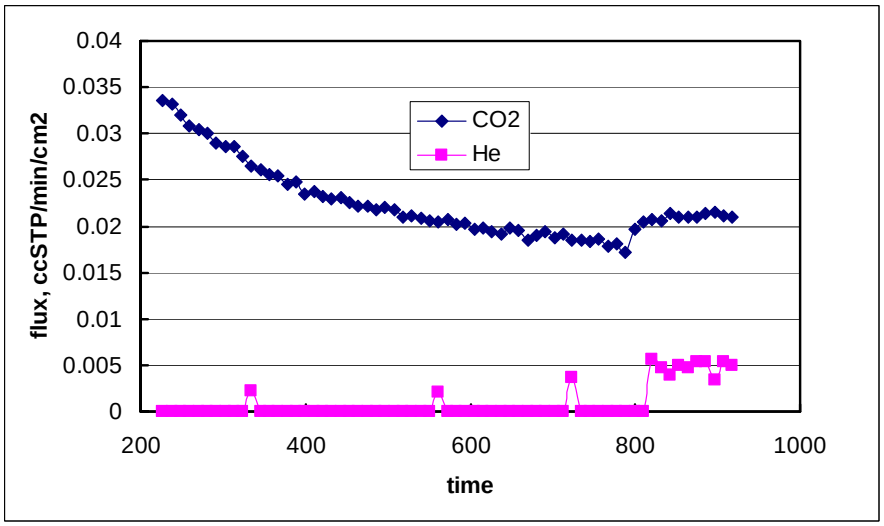

Figure 17. CO_2 Permeation for the Dual-Phase Membrane Prepared by ASU with 78.2% CO_2 and 21.8% He in Feed at 829°C

Oxygen was then introduced to the feed side to replace helium and CO_2 permeation testing continued with a feed gas composition of 50.8% CO_2 and 49.2% O_2. The results are shown in Figure 18 for both CO_2 and O_2 fluxes. The O_2 flux appeared to be about half of the CO_2 flux, which follows the reaction stoichiometry. After about 5 hours of operation, the CO_2 flux was about 4 or 5 times higher than that without O_2 in the feed, similar to what was observed at 752°C in Figure 15 and 16. The increase of the CO_2 flux by the use of O_2 in the feed is consistent with what the ASU team observed, at least qualitatively. However, O_2 is not expected to be present in the syngas stream generated from coal gasification systems. The data can only be used to help understand the transport mechanism for this type of dual-phase membrane.

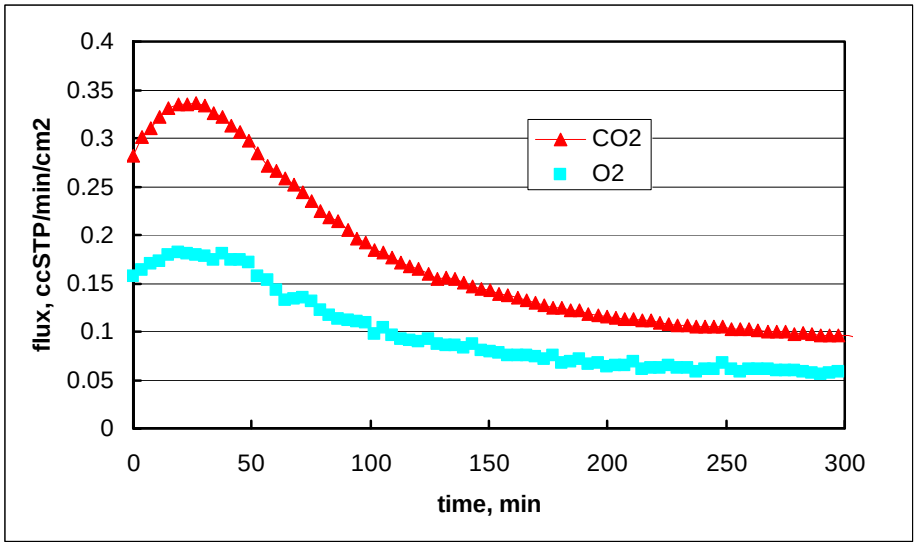

Figure 18. CO_2 Permeation for the Dual-Phase Membrane Prepared by ASU with 50.8% CO_2 and 49.2% O_2 in Feed at 829°C

Task 5.0 – Prepare and Test Proton-Conducting Membranes

Testing of hydrogen transport membrane (GTI)

Pd-Cu alloy foils, 99.9% purity and about 1 mm thick, were obtained from ACI Alloys. Circular membranes were cut from as-received foil sheets. The membranes were cleaned and sealed to the test cell using the glass-based sealant material. The tests were conducted with a 50/50 H_2/He feed containing 1,000 ppm H_2S at a temperature of 850°C and ambient pressure. Nitrogen was used in the permeate side as a sweep gas, which was sent to a GC for gas analysis.

Dual-phase membrane for H_2S permeation

A porous stainless steel support disk was infiltrated with molten carbonate by heating the powders and the disk together to a temperature of about 750°C. The stainless disk had a diameter of 2.22 cm, a thickness of 0.16 cm and a pore size of 0.5 µm. Helium leak check at room temperature confirmed that the pores of the membrane disk were completely blocked by the carbonate salts. High temperature H_2S permeation tests using glass-based sealant were then conducted.

Permeation tests were conducted with a gas feed consisting of 33.6% CO_2, 8.4% He, 57.6% H_2 and 0.4% H_2S at temperatures between 820° and 850°C and a pressure of 1 atm. In the permeate side, H_2 was used as a sweep gas to react with any sulfide ion that permeated through the membrane to formH_2S. Without H_2 purge, the sulfide ions would combine to form sulfur vapor. The permeate stream was sent to GC for analysis. The flow rate of H_2 sweep gas was 100 cc/min.

CO_2 permeation for ASU membrane

The CO_2-selective membranes prepared by ASU did not contain a metal phase of stainless steel as did those prepared at GTI. ASU's dual-phase membranes were fabricated by liquid infiltration of molten carbonate into an oxidation-resistant ceramic phase. The membranes were characterized by XRD as well as He permeation at room temperature.

CO_2 permeation testing was conducted in GTI's high-temperature permeation unit using the sealing material supplied by ASU. The membrane cell was first heated to about 920°C in CO_2 atmosphere to melt the sealant material. The presence of CO_2 in both feed and permeate sides prevented any possibility of decomposition of carbonates. Almost no He could be measured on the permeate side, indicating a very good seal as well as the nonporous characteristics of the membrane. The temperature was then decreased to 750°C or 829°C for CO_2 permeation testing. Nitrogen with a flow rate of 100 cc/min was used as a sweep gas in the permeate side. Tests were conducted with feed gas without the presence of oxygen, 78.2% CO_2 and 21.8% He and with the presence of oxygen, 50.8% CO_2 and 49.2% O_2. The pressure of the test was 0.34 bar.

Dual Phase Membrane (Arizona State University)

High-temperature permeation/separation experiments were conducted to confirm the CO_2 separation capabilities of the dual-phase membranes with $La_{0.6}Sr_{0.4}Co_{0.8}Fe_{0.2}O_{3-\delta}$ (LSCF6482) supports infiltrated with a Li/Na/K molten carbonate mixture (42.5/32.5/25.0 mole %). Briefly recall that in the presence of an electron, CO_2 and O_2 will react to form carbonaceous, CO_3^{2-}, as shown:

$$CO_2 + \frac{1}{2}O_2 + 2e^- \longleftrightarrow CO_3^{2-}$$

CO_3^{2-} is mobile in the molten carbonate phase. Separation is driven by the partial pressure gradient of CO_2 between the upstream and downstream sides of the membrane. Once CO_3^{2-} reaches the downstream side of the membrane, the electrons are released back into the support and circulated toward the upstream side of the membrane. The CO_3^{2-} ion decomposes on the downstream side to release CO_2 and O_2 on the permeate side. Past research has shown that the LSCF6482 material has suitable characteristics (conductivity, stability, etc.) for use as the support material.

Initially, the idea was to use graphite gaskets to seal the membrane. However, this was found to be a problem for two reasons. First, the graphite gaskets required a great deal of compression to form a seal. This was a problem because the ceramic supports were unable to withstand the amount of pressure required to form an adequate seal. Secondly, even if the membrane would seal, the graphite gasket would not last long at high temperatures in the presence of oxygen. As a result, a new method to seal the dual-phase membrane at high temperature was sought.

The 'new' sealing material was composed of 50% ground Pyrex beaker glass, 40% LSCF6482 powder (sintered at 900°C) and 10% $NaAlO_2$. The sealing powder was mixed with DI water to create a thick paste with a 'ketchup-like' consistency. The paste was applied to the 2.54 cm OD quartz tube and membrane interface to form the seal. The seal was allowed to dry in air for approximately 2 hours, after which a thin piece of parafilm was loosely placed over the top of the tube and left overnight. The following day, the parafilm was removed. The seal, although firm, was still somewhat damp. Sandpaper (800 SiC grade) was gently rubbed along the outside portion of the seal to produce a smooth surface. In addition, this action created more "wiggle" room for the quartz tube while it is in the high-temperature apparatus. A schematic of the high temperature permeation apparatus used for the experiments is shown in Figure 19.

Due to the presence of glass in the sealing material, it was preferable to heat the system to 900°C to allow the glass to soften and set to form a leak-free seal. However, it was already known that when heated in air at temperatures in excess of 700°C, the stability of the membrane decreases considerably. TGA-DSC experiments were performed on an infiltrated LSCF6482 membrane to look for possible changes at 750°C in air. Figure 20 shows the weight change of the infiltrated membrane as a function of temperature.

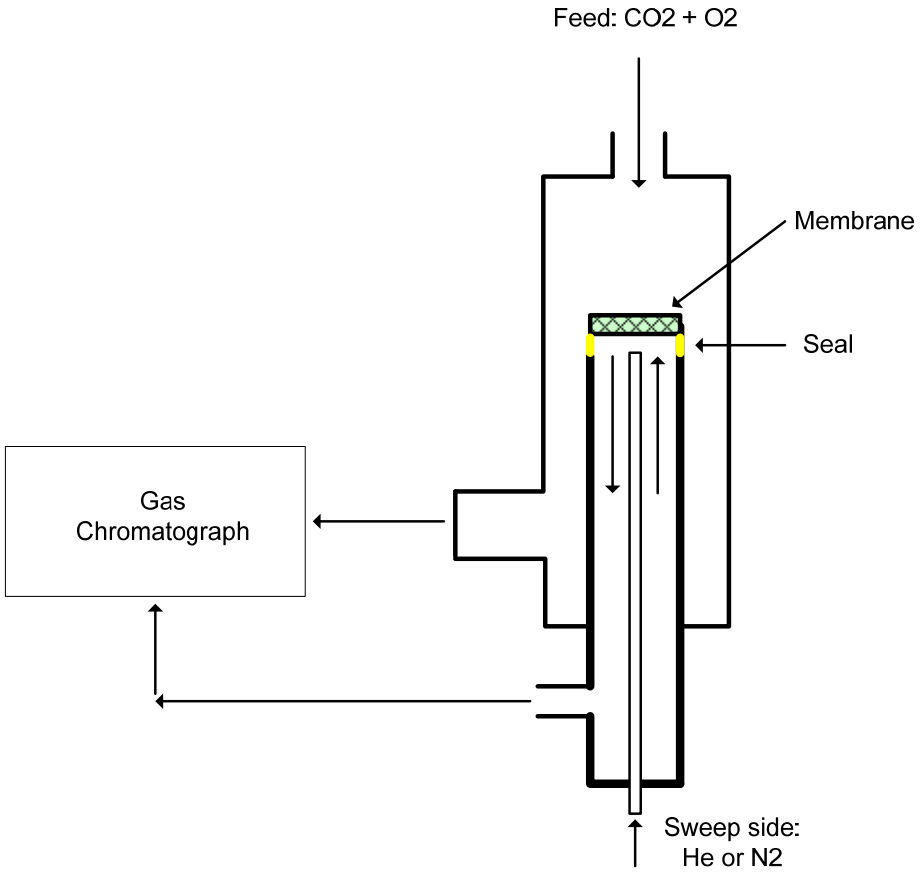

Figure 19. High Temperature Permeation Apparatus for High Temperature CO_2 Separation

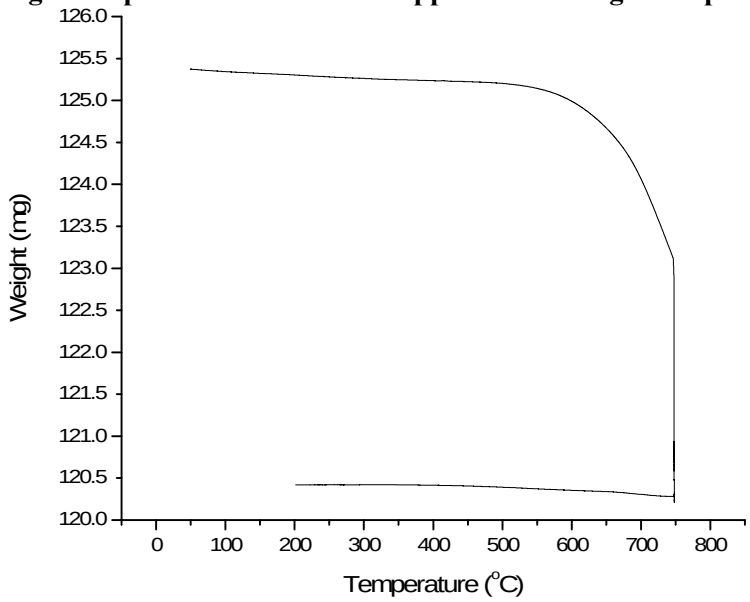

Figure 20. TGA-DSC of Infiltrated LSCF6482 Membrane (kept at 750°C for 5 hrs)

It is clear that the membrane decreases in weight rather substantially if it is kept at 750°C. It was postulated that the decrease in weight was a result of molten carbonate decomposition. To confirm this assumption, a TGA-DSC experiment was conducted on just the molten carbonate mixture (Li/Na/K). The result is shown in Figure 21, which appears similar to the result in Figure 20.

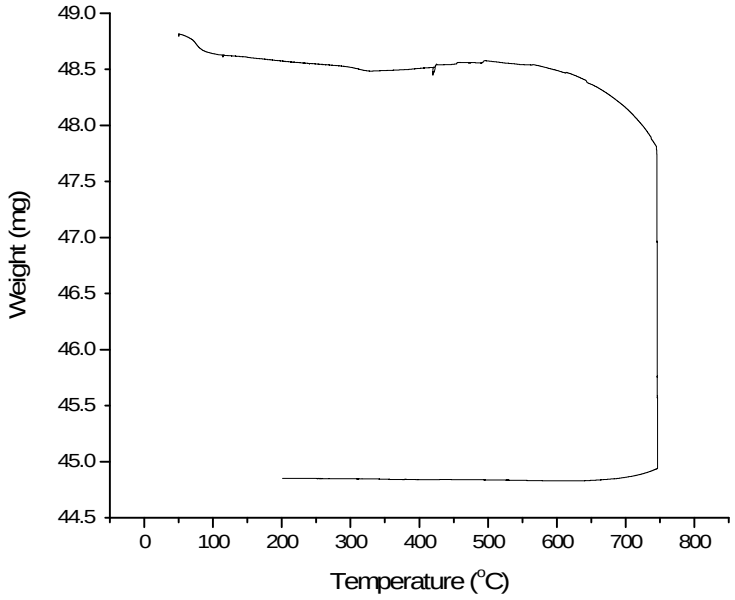

Figure 21. TGA-DSC of Molten Carbonate Mixture (kept at 750°C for 5 hrs)

High-temperature permeation experiments conducted on membranes heated in air for long periods of time produced no viable results. During ASU's discussions with GTI, it was noted that the stability of the membrane could be better maintained when the membrane was heated in a CO_2 atmosphere. Two such experiments were conducted.

The infiltrated membranes were sealed to the 2.54 cm OD alumina tube and heated with a ramp rate of 1°C/min to 915°C. Heating to this temperature allowed for the Pyrex glass in the seal material to soften, forming a seal with little to no apparent leakage of the feed/sweep gases. During heating, the feed and permeate sides were exposed to CO_2 at rates of 100 ml/min. Upon reaching 915°C, the system was held at constant temperature for about an hour to allow the seal to set. Afterwards, the temperature of the system was decreased at a ramp rate of 2°C/min to the desired value. The details of each experiment are discussed below:

Experiment #1:

After reaching a target of 915°C and holding at temperature for one hour, the system temperature was decreased to 850°C. Upon reaching 850°C, CO_2 on the permeate side (which was used to "protect' the membrane) was changed to N_2 (100 ml/min; sweep gas). Helium, at a rate of 100 ml/min, was added to the feed along with the CO_2 that was already flowing.

- Feed: CO_2 and He (100 ml/min, each)
- Sweep: N_2 (100 ml/min)

Tests were conducted to determine the effect of CO_2 flux withoutO_2. Afterwards, the He feed gas was switched to O_2:

- Feed: CO_2 and O_2 (100 ml/min, each)
- Sweep: N_2 (100 ml/min)

Two readings each (CO_2/He and CO_2/O_2 feeds) were taken at 850º, 800º and 750°C (in that order). The CO_2 flux for the CO_2/He and CO_2/O_2 high temperature experiments are summarized in Table 2.

Table 2. CO_2 Flux in High Temperature Permeation Test #1

Temperature (°C)	CO_2 flux for CO_2/He feed ($ml/cm^2 \cdot min$)	CO_2 flux for CO_2/O_2 feed ($ml/cm^2 \cdot min$)	Net Difference in CO_2/He, CO_2/O_2 flux ($ml/cm^2 \cdot min$)
750	0.208	0.317	0.109
800	0.508	0.623	0.115
850	0.463	0.587	0.124

The data indicate that the membrane does work and shows improved flux when O_2 was introduced. The main problem encountered during this experiment was that it was not possible to determine the leakage rate of the feed gases because He was used as the inert feed gas and also gas chromatograph (GC) carrier gas. Consequently, the leakage of He could not be detected by the GC.

Experiment #2:

After reaching a target of 915°C and holding temperature for one hour, the system temperature was decreased to 550°C at 2°C/min, while maintaining a CO_2 flow of 100 ml/min on both sides of the membrane. After reaching 550°C, CO_2 on the permeate side was changed to He (100 ml/min; sweep gas). N_2 at a rate of 100 ml/min was added to the feed.

- Feed: CO_2 and N_2 (100 ml/min, each)
- Sweep: He (100 ml/min)

Permeation was tested to determine the effect of CO_2 permeance withoutO_2. Subsequently, N_2 in the feed was shut off and then changed to O_2:

- Feed: CO_2 and O_2 (100 ml/min each)
- Sweep: He (100 ml/min)

The tests indicate that the addition of O_2 improves the permeance of CO_2 through the membrane.

On a related topic, knowing that the LSCF6482 membranes and concept works, ASU has investigated new materials with high O_2 ion conductivity to use as the support for the dual-phase membrane. In short, the idea is to be able to permeate CO_2 through the dual-phase membrane without having to introduce O_2 into the feed. Instead, $O_2^{=}$ ions in the material would be used as the source of O_2 for the reaction:

$$CO_2 + \frac{1}{2}O_2^{=} \longleftrightarrow CO_3^{2-}$$

Table 3 shows a brief list of the materials that were investigated and their $O_2^{=}$ conductivity. The list includes a good mix of materials closely related to the LSCF6482 and completely unrelated materials based on stabilized bismuth oxides.

Table 3. High Oxygen Ion Conducting Materials for Potential Use as the Dual-Phase Membrane Support Material (7)

Material	$O_2^{=}$ conductivity (S/cm)
$La_{0.2}Sr_{0.8}Co_{0.2}Fe_{0.8}O_{3-\delta}$	0.62
$La_{0.2}Sr_{0.8}Co_{0.8}Fe_{0.2}O_{3-\delta}$	0.87
$Y_{0.16}Bi_{0.64}O_2$	~3
$Y_{0.6}Bi_{0.1.4}O_3$	~10
$Cu_{0.1}Y_{0.6}Bi_{1.3}O_3$	~10

The first step was to determine stability and whether or not the materials listed were compatible with molten carbonate at high temperatures.

Task 6.0 – Modeling and Process Simulation

Simplified Model

To understand the advantages of the complementary membrane reactor process, a simplified model was developed to evaluate its performance. The membrane shift reactor is modeled as a water-gas-shift-reactor and a membrane separation unit with part of its non-permeate stream or retentate recycled to the shift reactor. Thermodynamic equilibrium is assumed for the shift reaction. The hydrogen separator is modeled as component splitter, where H_2 is produced at a pressure of 1.03 bara (14.65 psia). By setting the hydrogen partial pressure in the retentate stream slightly higher than the permeate pressure, at 1.10 bara (15.65 psia), the H_2 flux from the hydrogen separator can be calculated.

In a real membrane shift reactor, simultaneous reaction and separation would be taking place. This is accounted for by the recycle stream from the retentate. Without any recycle, the shift

reactor and the membrane separator are not integrated. On the other hand, with 100% recycle, the simulation scheme becomes a Continuous Stirred Tank Reactor (CSTR), with simultaneous H_2 removal from the reactor. In this work, the recycle stream is assumed to be 80% of the retentate. The above process scheme was simulated using the HYSYS process simulator. Although hydrogen is used as an example in Figure 22, the CO_2 membrane shift reactor can be modeled in the same way.

For the complementary membrane reactor process, the simulation flow diagram is shown in Figure 23. The retentate stream from the CO_2 membrane shift reactor is sent to the H_2 membrane shift reactor, following the same assumptions as in Figure 22.

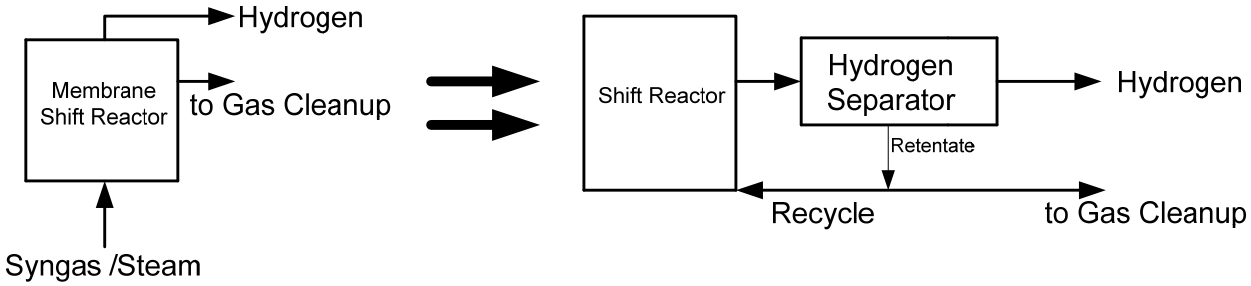

Figure 22. Modeling of Membrane Shift Reactor

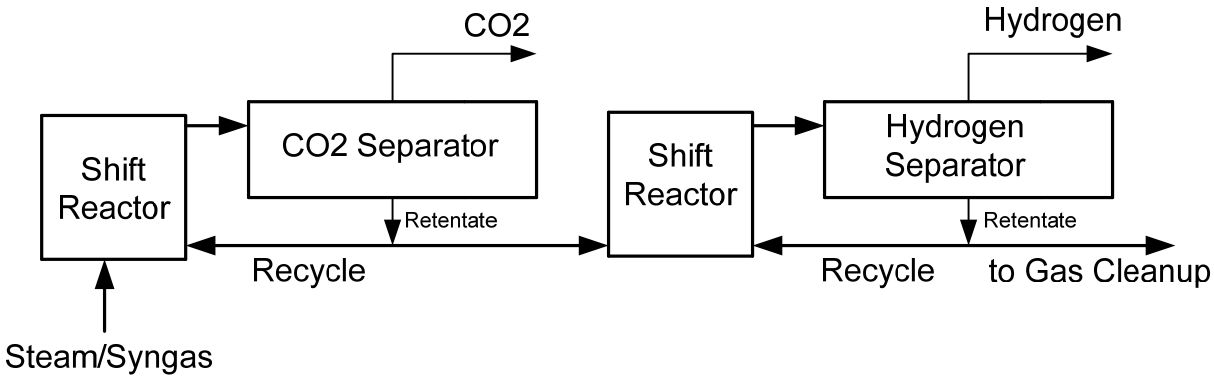

Figure 23. Modeling of Complementary Membrane Shift Reactor

Improved Model

The above simplified models do not allow the estimation of membrane transport area, which is an important parameter for evaluating the feasibility of the proposed membrane reactor technology. An improved version of the equilibrium model was therefore developed. The model still consists of a component splitter and an equilibrium shift reactor in the HYSYS process simulator, however instead of recycling the retentate stream from the component splitter back to

the shift reactor, the membrane reactor was modeled as a series of component splitters and shift reactors to simulate a more realistic plug flow reactor, as shown in Figure 24 for the complementary membrane reactor.

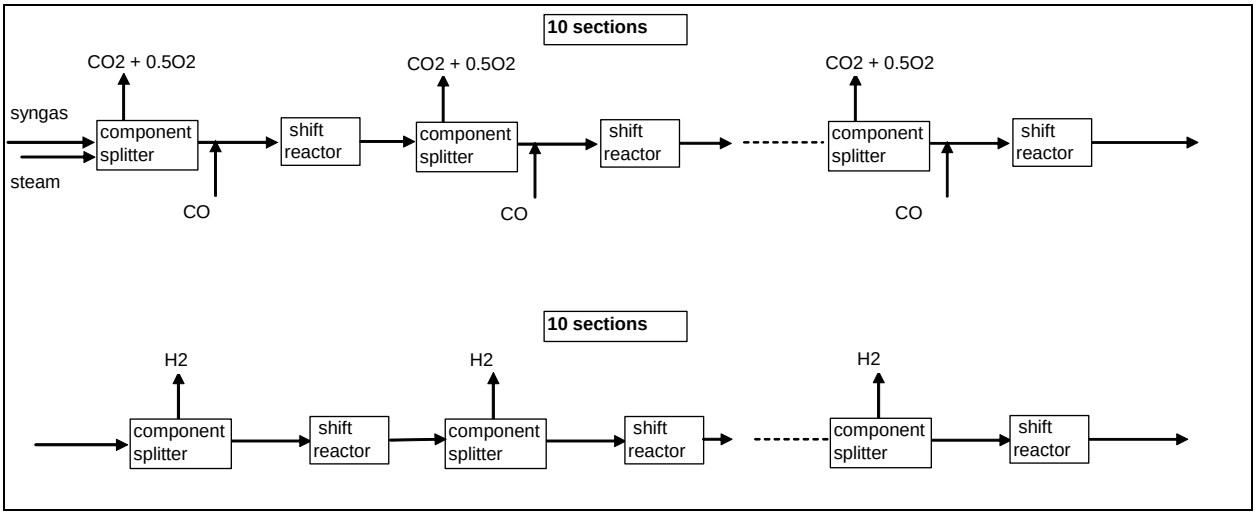

Figure 24. HYSYS Model of Complementary Membrane Reactor

The amounts of CO_2 or H_2 that permeate through the membrane are based on permeation or a transport model and the measured conductivity or permeability data generated in this project.

Transport Model for CO_2-Selective Dual-Phase Membrane

CO_2 transport for the dual-phase membrane follows the following mechanism:

Feed side: $2CO_2 + 2\ e^- \rightarrow CO + CO_3^{2-}$ (1)

Permeate side: $CO_3^{2-} \rightarrow CO_2 + 1/2O_2 + 2\ e^-$ (2)

The CO_2 undergoes a charge-transfer reaction on the upstream membrane surface to form charged CO_3^{-2}. The charged carbonaceous species diffuses toward the other side of the membrane and is converted to molecular CO_2 in a reverse reaction on the downstream membrane surface. During the process, the electrons move in the opposite direction through the metal support. As shown in the Appendix, the neutral flux for CO_2 in this case can be related to the conductivities of the two charged species in the dual-phase membrane:

$$J_{CO_2} = -\frac{3RT}{8F^2L}\int_{P_1}^{P_2}\frac{\sigma_{ion}\sigma_{el}}{(\sigma_{ion}+\sigma_{el})}d\ln P_{CO_2} \quad \textbf{(3)}$$

where P_{CO2} is the partial pressure of CO_2, P_1 is the CO_2 pressure at the feed side and P_2 is the CO_2 pressure at the permeate side. At the permeation temperature, the ionic conductivity of CO_3^{2-} in the molten carbonate phase (0.5~2 S/cm) is much smaller than the electronic conductivity for the stainless-steel phase (~10^4 S/cm). Therefore, the conductivity contribution term in eq. 3 can be

reduced to ionic conductivity only. Considering the porosity (ε) and tortuosity (τ) of the metal support, and assuming CO_2 pressure-independent ionic conductivity, integration of eq. 3 gives CO_2 permeance:

$$J_{CO_2} = -\frac{3RT}{8F^2L}\sigma_{ion}\frac{\varepsilon}{\tau}\ln\frac{P_2}{P_1} \quad \textbf{(4)}$$

In a simplified form, the CO_2 flux can be related to temperature T, pressure gradient of CO_2 $\ln(P_2/P_1)$, membrane thickness L, and a constant K, which is related to the membrane property such as ionic conductivity, porosity and tortuosity.

$$J_{CO_2} = -K\frac{T}{L}\ln\frac{P_2}{P_1} \quad \textbf{(5)}$$

$$\textbf{where } K = -\frac{3R}{8F^2}\sigma_{ion}\frac{\varepsilon}{\tau} \quad \textbf{(6)}$$

Transport Model for H_2-Selective Metallic Membrane

Hydrogen permeation in Pd-Cu membrane generally follows Sievert's law:

$$J_{H_2} = M\frac{P_{feed}^{0.5} - P_{perm}^{0.5}}{L} \quad \textbf{(7)}$$

where M is the membrane permeability, L is the membrane thickness, P_{feed} is the H_2 pressure at the feed side and P_{perm} is the H_2 pressure at the permeate side.

The value of K in eq. 6 was determined from the CO_2 permeation data measured in this project with actual operating temperature, pressures, and membrane thickness. Similarly, the value of M was determined from the H_2 permeation data measured in this project. The experimental values of K and M were then used to calculate the amounts of H_2 or CO_2 in the improved model. The membrane thickness was assumed to be 20 μm, which is considered achievable with current fabrication technologies. The required transport area for each component splitter in Figure 24 was determined by setting the CO_2 or H_2 partial pressure in the last retentate stream slightly higher than the permeate pressure. The permeate pressure is 1.38 barg (19.6 psig) for H_2 and 0.97 barg (13.8 psig) for CO_2 because half mole of O_2 is also generated for each mole of CO_2 generated in the permeate side according to eq. 2. Because CO is also generated in the feed side, for each mole of CO_2 permeated through the membrane, one mole of CO is added to the retentate stream of each component splitter in Figure 24, with 2 moles of CO_2 actually removed from the component splitter. In Figure 24, ten sections of component splitter and shift reactors are used for the CO_2 membrane reactor and the H_2 membrane reactor.

A variation of the complementary membrane reactor configuration is to alternate the CO_2-selective membrane reactor with the H_2-selective membrane reactor as shown in Figure 25. The advantage of this configuration is to increase the CO_2 concentration in the second section of the CO_2-selective membrane reactor due to additional shift reaction in the first H_2-selective

membrane reactor. Other possible configurations can include placing the H_2-selective membrane reactor in front of the CO_2-selective membrane reactor.

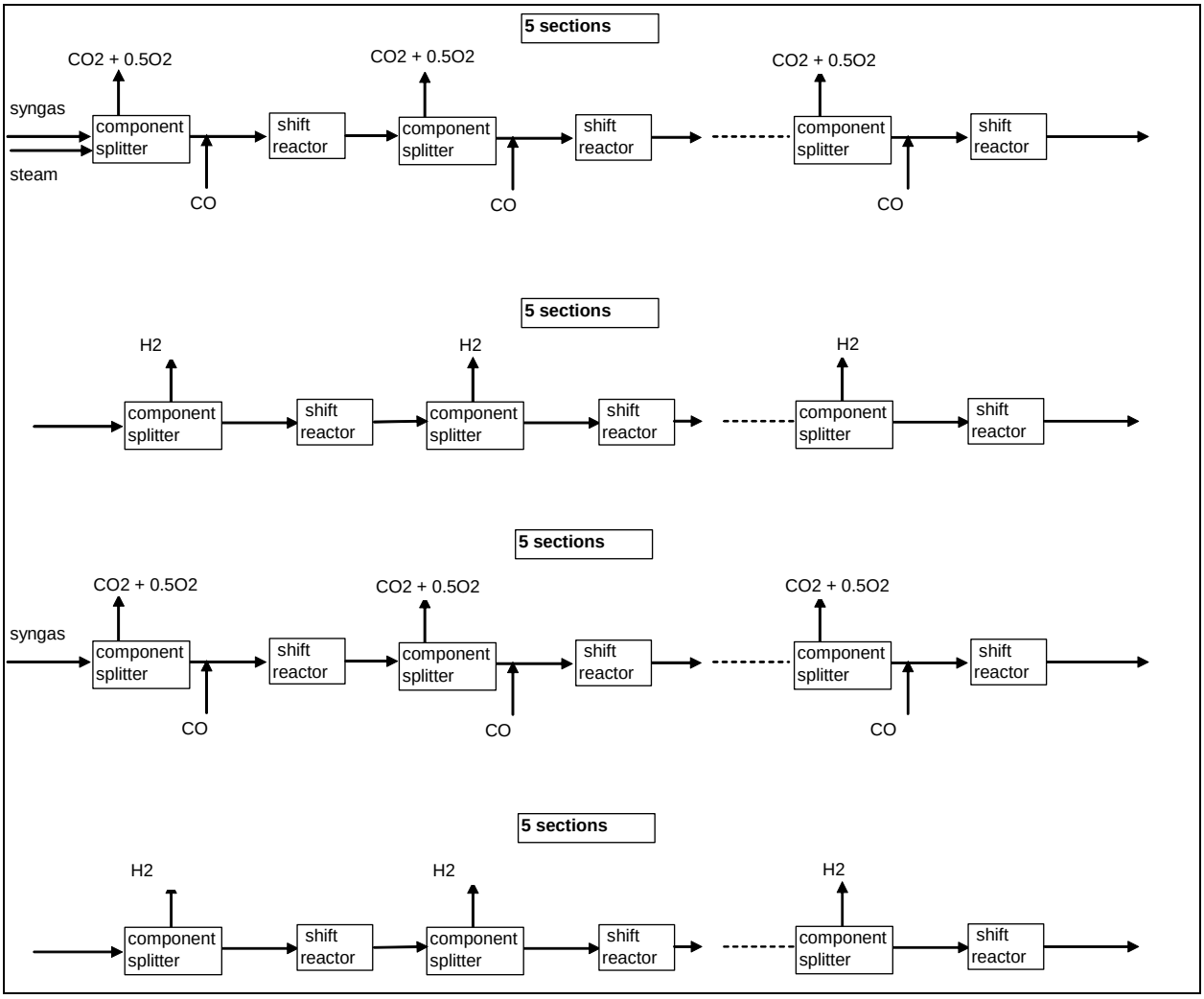

Figure 25. HYSYS Model for Variation of Membrane Reactor

Simplified Model

The calculations are based on a coal feed rate of 45,360 kg/hr (100,000 lbs/hr) of Illinois No. 6, operating at a temperature of 1000ºC (1832ºF) and a pressure of 30 atm using GTI's U-GAS® fluidized-bed gasifier model. Because only major components, carbon (C), hydrogen (H), and oxygen (O) are utilized for the mass balance of this analysis, the syngas compositions entering the membrane reactors are normalized to the following: 32.3% CO, 12.1% CO_2, 33.1% H_2, 22% H_2O, and 0.5% CH_4. Simulations were performed for three membrane reactor processes to compare their performances. The processes simulated were 1) the complementary membrane reactor process with both CO_2-membrane and H_2-membrane, 2) the CO_2-selective membrane only and 3) the hydrogen-selective membrane only.

Figure 26 shows H_2 produced for the three membrane reactor processes at different temperatures. For the CO_2-membrane only process, an additional H_2 purification unit will be required to obtain a high purity H_2 product. This undefined unit is assumed to recover 90% of H_2 from the membrane retentate stream. As can be seen from Figure 26, use of the complementary membrane reactor process can produce more H_2 product than the other two processes. This is mainly due to the increased CO conversion by the shift reaction since both the reaction products, H_2 and CO_2 are removed. Because of the exothermic nature of the shift reaction, lower temperatures favor the production of hydrogen, as expected.

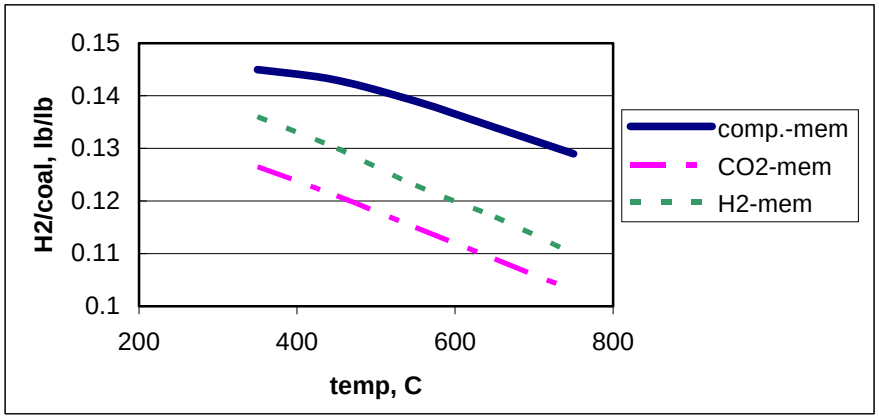

Figure 26. Comparison of Hydrogen Production for Three Different Membrane Reactor Processes from Simulation

The amounts of CO_2 that can be removed from the three processes are compared in Figure 27. The amount of CO_2 removed by the CO_2-membrane process is the same as the complementary membrane reactor process; therefore, it is not shown in Figure 27. Again, a CO_2 purification unit will be needed to obtain a high purity CO_2 stream from the H_2-membrane process, because the retentate stream from the H_2-membrane process can only have a CO_2 concentration less than 89% (dry basis). Assuming 90% pure CO_2 can be recovered from this stream, the amounts of CO_2 removed actually are very close to those from the complementary membrane reactor process. However, purification of this CO_2-rich stream is not trivial. It requires the use of a CO_2-selective membrane that will produce a pure CO_2 product, while also providing a synergetic

effect to the H_2 membrane for increasing the CO conversion in the shift reactor, as is demonstrated in the complementary membrane reactor process.

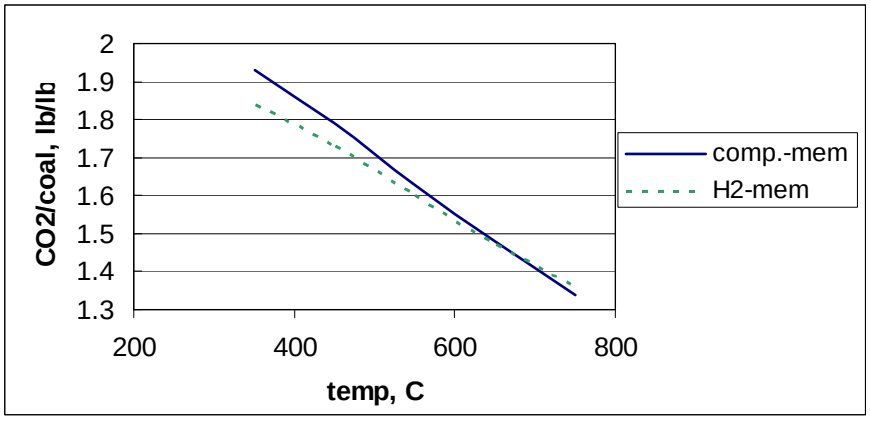

Figure 27. Comparison of CO_2 Removed for Three Different Membrane Reactor Processes from Simulation (Complementary and CO_2 plots are identical)

Figure 28 shows the comparison of the gas flows of the retentate streams from the three membrane reactor processes. After separating CO_2 and H_2 from the syngas, the remaining gas flow from the complementary membrane reactor process is much lower than the other two membrane reactor processes. If this retentate stream needs further conditioning before it is sent to a gas turbine or other energy recovery device, the equipment size will be significantly reduced.

One of the disadvantages of the membrane separation process is that product recompression may be required if the desired product is the permeate stream. It is not clear whether the benefits of the complementary membrane reactor process can outweigh the penalty of compression cost. A more detailed economic analysis will be required.

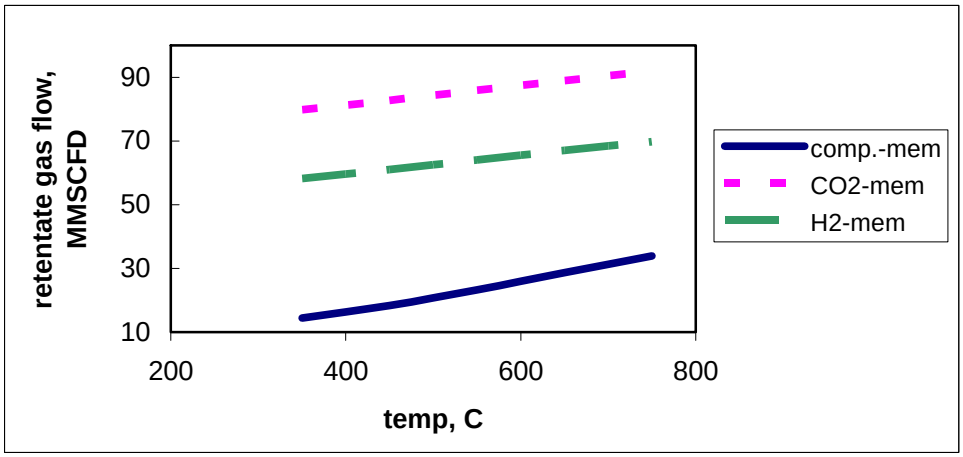

Figure 28. Comparison of Retentate Gas Flows for Three Different Membrane Reactor Processes from Simulation

Improved Model

The calculation basis for the improved model was the same as that used for the simplified model, i.e., a coal feed of 45,360 kg/h (100,000 lbs/hr) of Illinois No. 6, gasifier operating at a temperature of 1000ºC (1832ºF), and a pressure of 30 atm using GTI's U-GAS® fluidized-bed gasifier model. To facilitate the water-gas-shift reaction, an additional 1,000 kg mole/hr of steam was added to the front of the membrane reactor. Figure 29 shows the permeated CO_2 flows and the CO_2 mole fractions at the different locations of the CO_2-selective membrane reactor, using the configuration shown in Figure 24. While CO_2 mole fraction starts to decrease inside the reactor, the driving force from the CO_2 partial pressure also decreases, which reduces the CO_2 permeation. However, due to the shift reaction, the H_2 mole fraction increases at the end of the CO_2-membrane section or the beginning of the H_2-membrane section. Figure 30 shows the permeated H_2 flows and the H_2 mole fractions at the different locations of the H_2-selective membrane reactor.

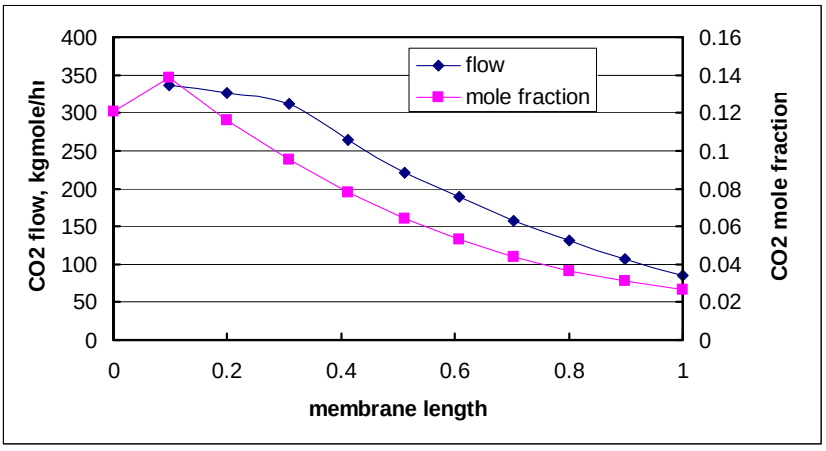

Figure 29. CO_2 Flow and Mole Fraction vs Membrane Length

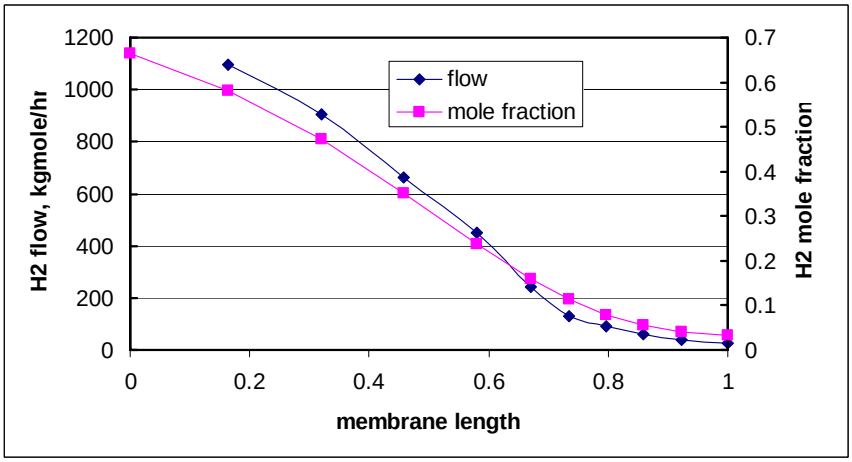

Figure 30. H_2 Flow and Mole Fraction vs Membrane Length

Using the configuration shown in Figure 7, the CO_2 and H_2 permeated flows and mole fractions in the membrane reactors are shown in Figures 31 and 32 respectively. The CO_2 membrane reactors are placed in the first and the third sections of the single membrane reactor while H_2 membrane reactors are in the second and the fourth sections. The CO_2 mole fractions in the CO_2 membrane reactor are generally higher than those in Figure 29. However, the hydrogen mole fractions are lower in Figure 32 than in Figure 30.

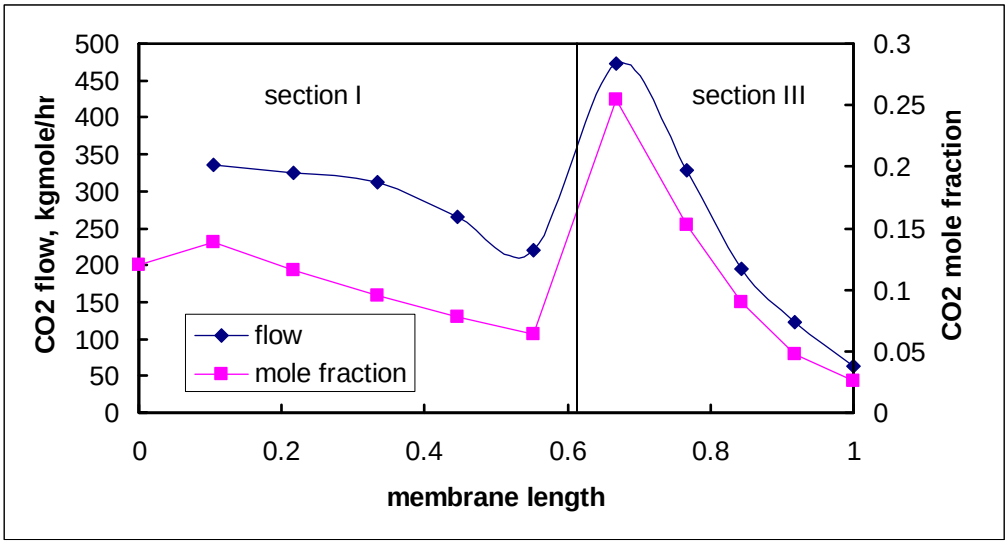

Figure 31. CO_2 Flow and Mole Fraction vs Membrane Length for Model Variation

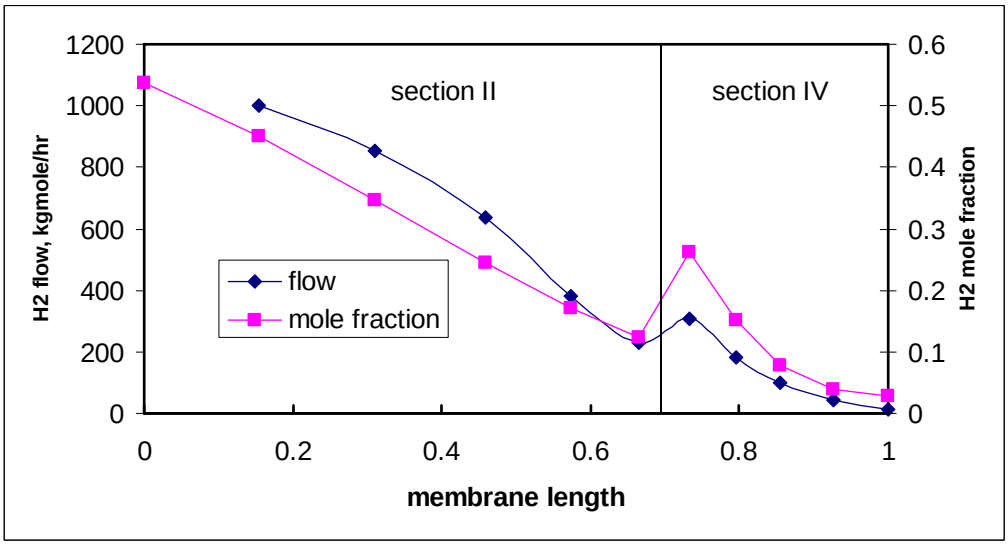

Figure 32. H_2 Flow and Mole Fraction vs Membrane Length for Model Variation

Table 4 summarizes the overall performances for the three cases studied. Cases I and II are based on the configuration shown in Figure 24 with two different steam flow rates. Case III is based on the configuration shown in Figure 25. Use of more steam promotes more shift reaction.

As a result, more CO_2 and H_2 are generated from the membrane reactors and the CO content is lower in the retentate stream of the membrane reactor.

Table 4. Membrane Reactor Results Summary

		Case I	Case II	Case III
Steam, kg-mole/hr		1800	1000	1000
CO_2 mem. Section	CO_2 flow, kg-mole/hr	1255	1064	1320
	area, m^2	340,000	305,000	282,000
H_2 mem. Section	H_2 flow, kg-mole/hr	4334	3700	3750
	area, m^2	2970	2440	2790
Retentate flow	kg-mole/hr	1280	1290	980
Retentate mole fraction	CH_4	0.03	0.02	0.03
	H_2	0.03	0.03	0.03
	H_2O	0.17	0.03	0.00
	CO	0.14	0.49	0.87
	CO_2	0.63	0.43	0.08

The modeling work has identified where additional work is required. As is evident from the results in the table, the major hurdle is the large area required for the CO_2 membrane. There are two approaches possible The first would be to seek a different material for the membrane that can achieve higher fluxes/separations. The other would be to try to modify the existing materials that are known to be selective for CO_2 separation. The goal of either approach would be to increase the flux of CO_2 through the membrane.

The conceptual process flow diagram for the membrane reactor process is shown in Figure 33. The coal is first gasified to produce a syngas. The gasifier yields were estimated by using the model for GTI's UGAS® process. The coal used was a typical Illinois No. 6. The conditions

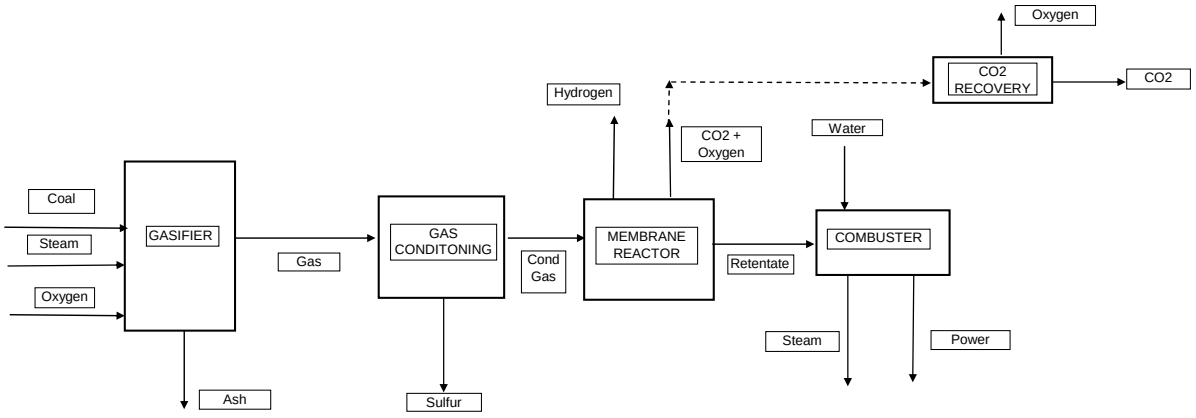

Figure 33. Overall Process Flow Diagram for Membrane Reactor Process

used to model the gasifier were a temperature of 1000ºC (1832 ºF) and a pressure of 30 atm and a coal feed rate of 45,360 kg/hr (100,000 lbs/hr). The next step after the gasifier was to remove

trace contaminants such as H_2S, HCN, and COS. Currently, this would require cooling the gas if conventional technology were used to accomplish this task. However, developing hot gas technologies may make the cooling step unnecessary. In the event that the gas will require cooling, steam can be utilized and generated in the heat removal step. In addition to the trace contaminants, particulates that are not trapped by the cyclones will require removal, probably by either ceramic or metallic filters.

After the gas is conditioned, it enters the membrane reactor. Two permeate streams are produced, one containing H_2 and the other containing CO_2 and O_2. The gases can then be sent to other units where they will be used. In the case of the CO_2 stream, additional processing may be required to remove the O_2. The remaining stream produced in the membrane reactor is the retentate. The heating value of this gas makes it a candidate for combustion. The heat from the combustion process can then be used to raise steam or heat feed gases used in the overall process. In addition, the pressure of this stream is sufficiently high that it can be used to generate power. Options such as the extent of heat recovery at different points in the process, the extent of gas conditioning, the use of the CO_2 stream and the amount of power generation, would have to be pursued to develop a more detailed and efficient process flow diagram.

CONCLUSIONS AND RECOMMENDATIONS

Membrane disks using the technique of powder pressing and high-temperature sintering were successfully fabricated, using metal oxide or metal carbonate materials. Experiments on CO_2 permeation testing were also performed in the temperature range of 790º to 940°C for the metal carbonate membrane disks. However, no CO_2 permeation rate could be measured, probably due to very slow CO_2 diffusion in the solid state carbonates.

To improve the permeation of CO_2, membranes with liquid or molten carbonates were fabricated. Several different types of dual-phase membranes were tested for their CO_2 permeation in reducing conditions without the presence ofO_2. Although the flux was quite low, on the order of 0.01-0.001 cc STP/cm^2/min, the selectivity of CO_2/H_2 was almost infinite at a temperature of about 800°C. More tests should be conducted to confirm the preliminary but encouraging results for this approach.

For tubular membranes that were fabricated by solution impregnation with metal carbonates, difficulties were encountered in removing the impurity salts that were trapped inside the porous support tube. The membrane tube would continue losing its weight after being heated to 500°C in air and would not maintain its nonporous characteristics. This approach was abandoned.

In the area of H_2 transport membrane, hydrogen permeation of a commercial Pd-Cu alloy foil was tested at 850°C for continuous operation of about 2 weeks. There was no performance degradation observed relative to H_2 flux, which is a good indication of its thermal stability at this high temperature. A permeation test was also performed with a feed gas containing 1000 ppm H_2S, 50% H_2 and balance He at 850°C. No H_2 flux decline was observed after 8 hours of operation. The test results indicate that the Pd-Cu alloy membrane possesses good thermal stability and sulfur tolerance in the temperature range of interest in this project, 750º to 900°C.

Mixed ionic/electronic conducting membranes that contain a carbonate phase and a metal phase were successfully tested for H_2S permeation. The measured H_2S flux was on the order of 0.01-0.03 cc STP/cm^2/min. The flux of H_2S was considerably higher than CO_2 with a H_2S/CO_2 selectivity approaching 2000. This type of membrane can be used for front-end sulfur removal in the single membrane reactor configuration. The sulfide ion conducting membrane can also directly produce elemental sulfur downstream of the membrane, which can eliminate the Claus plant that is typically needed with other sulfur removal technologies.

A different type of dual-phase membrane prepared by Arizona State University (ASU) was also tested at GTI for CO_2 permeation. The measured CO_2 fluxes were 0.015 and 0.02 cc STP/cm^2/min at 750 and 830°C, respectively. These fluxes were higher than the previous flux obtained (~0.01 cc STP/cm^2/min) using the dual-phase membranes prepared by GTI. Further membrane development should be conducted to improve the CO_2 flux.

- The permeation experiments indicate that the addition of O_2 does improve the permeance of CO_2 through the membrane.

- The membrane shift reactor process shows promise as a means to simplify the production of a clean stream of H_2 and a clean stream ofCO_2.

- Additional development work should address the large area required for the CO_2 membrane.

- A more detailed process flow diagram should be developed that includes integration of cooling and preheating feed streams as well as particulate removal so that steam and power generation can be optimized.

REFERENCES

1. D. Weaver and J. Winnick “Electrochemical Removal of H_2S from Hot Gas Stream”, Journal of Electrochemical Society, Vol. 134, No(10) 2451 (1987)
2. A. Burke, J. Winnick, C. Xia and M. Liu “Removal of Hydrogen Sulfide from a Fuel Gas Stream by Electrochemical Membrane Separation”, Journal of Electrochemical Society, Vol.149 (11) D160 (2002)
3. S.R. Alexander and J. Winnick “Electrochemical Polishing of Hydrogen Sulfide from Coal Synthesis Gas”, Journal of Applied Electrochemistry, 24 1092 (1994)
4. J.S. Robinson, D. S. Smith and J. Winnick “Electrochemical Membrane Separation of H2S from Reducing Gas Streams”, AIChE Journal, Vol. 44, No10 2168 (1998)
5. A. Burke, S. Li, J. Winnick, and M. Liu “Sulfur-Tolerant Cathode Material in Electrochemical Membrane System for H2S Removal from Hot Fuel Gas”, Journal of Electrochemical Society, 151 (7) D55 (2004)
6. S.J. Chung, J.H. park, D.Li, J.-I Ida, I. Kumakiri, and Jerry Y.S. Lin, “Dual-Phase Metal-Carbonate Membrane for High-Temperature Carbon Dioxide Separation” *Ind. Eng. Chem. Res.* 2005, 44, 7999-8006
7. Shuk, P., H.-D. Wiemhofer, U. Guth, W. Gopel, M. Greenblatt, “Oxide ion conducting solid electrolytes based on Bi_2O_3“, *Solid State Ionics*, 89 (1996) 179.

ABBREVIATIONS

atm	= atmosphere
barg	= pressure, gauge
cc	= cubic centimeter
cm	= centimeter
CSTR	= continuous stirred tank reactor
DI	= deionized
DSC	= differential scanning calorimeter
e.g.	= “exempli gratia”, for example
eqs	= equations
hrs	= hours
i.e.	= “id est”, that is
nm	= nanometer
STP	= Standard Temperature and Pressure of 760 mm Hg and 25 ºC
SEM	= scanning electron microsope/microscopy
TGA	= thermal gravimetric analyser/analysis
wt	= weight
XRD	= x-ray diffraction

Appendix[1]: Permeation Model for Metal-Carbonate Dual-Phase Membranes

The dual-phase membrane consists of a molten carbonate phase and a porous metal phase. Assuming that bulk diffusion is the rate-limiting step, the fluxes of the two charged species (CO_3^{2-} and electrons) in the bulk phase membrane are given:

$$\text{for } CO_3^{2-}: \quad J_1 = -\frac{\sigma_1}{z_1^2 F}(\nabla\mu_1 + z_1 F\nabla\phi_1) \qquad (\text{for } z_1 = 2) \quad \text{(A-1)}$$

$$\text{for electron:} \quad J_2 = -\frac{\sigma_2}{z_2^2 F}(\nabla\mu_2 + z_2 F\nabla\phi_2) \qquad (\text{for } z_2 = 1) \quad \text{(A-2)}$$

where $\nabla\mu_i$ and $\nabla\phi_i$ are the chemical potential and electric-field gradient, respectively, for species i and z_i is the charge number of species i (1 = CO_3^{2-}, 2 = electron). To avoid complexity, transport of the cations was neglected in the model.

Because no external current exists in the membrane, one has

$$z_1 J_1 + z_2 J_2 = 0 \quad \text{(A-3)}$$

Combining eqs A-1 to A-3 gives

$$J_1 = -\frac{\sigma_1\sigma_2}{(\sigma_1+\sigma_2)z_1^2 F^2}\left(\nabla\mu_1 - \frac{z_1}{z_2}\nabla\mu_2\right) \quad \text{(A-4)}$$

At equilibrium, reaction (1) becomes

$$2\nabla\mu_{CO_2} - \nabla\mu_{CO} = \nabla\mu_1 - 2\nabla\mu_2 \quad \text{(A-5)}$$

Inserting eq A-5 into equation A-4 yields

$$J_1 = -\frac{\sigma_1\sigma_2}{4(\sigma_1+\sigma_2)F^2}\left(2\nabla\mu_{CO_2} - \nabla\mu_{CO}\right) \quad \text{(A-6)}$$

Chemical potential (μ_i) and thermodynamic factor (f_i) were respectively defined as

$$\nabla\mu_i = \frac{RT}{C_i}\left(\frac{\partial \ln a_i}{\partial \ln C_i}\right)\nabla C_i \quad \text{(A-7a)}$$

$$f_i = \frac{\partial \ln a_i}{\partial \ln C_i} \quad \text{(A-7b)}$$

If one lets i = I for CO_2 and i = II for CO, the chemical potential gradient can be expressed as follows:

[1] S.J. Chung, J.H. park, D.Li, J.-I Ida, I. Kumakiri, and Jerry Y.S. Lin, "Dual-Phase Metal-Carbonate Membrane for High-Temperature Carbon Dioxide Separation" *Ind. Eng. Chem. Res.* 2005, 44, 7999-8006

$$\nabla \mu_{CO_2} = \nabla \mu_I = \frac{RT}{C_I}\left(\frac{\partial \ln a_I}{\partial \ln C_I}\right)\nabla C_I = \frac{RT}{C_I} f_I \nabla C_I \quad \text{(A-8)}$$

$$\nabla \mu_{CO} = \nabla \mu_{II} = \frac{RT}{C_{II}}\left(\frac{\partial \ln a_{II}}{\partial \ln C_{II}}\right)\nabla C_{II} = \frac{RT}{C_{II}} f_{II} \nabla C_{II} \quad \text{….(A-9)}$$

With $J_{CO2} = J_1$, combining eqs A-6-A-9 gives

$$J_{CO_2} = -\frac{\sigma_1 \sigma_2 RT}{4(\sigma_1 + \sigma_2)F^2}\left(2 f_I \frac{\nabla C_I}{C_I} + \frac{f_{II} \nabla C_{II}}{C_{II}}\right) \quad \text{(A-10)}$$

Because CO_2 generate CO in the molar ratio of 2:1 (CO_2/CO), the concentration gradient of the reactant in the membrane is expressed as follows:

$$\nabla C_I = -2\nabla C_{II} \quad \text{(A-11)}$$

From eqs A-10 and A-11, one has

$$J_{CO_2} = -\frac{\sigma_1 \sigma_2 RT}{4(\sigma_1 + \sigma_2)F^2}\left(2 f_I \frac{\nabla C_I}{C_I} - \frac{f_{II} \nabla C_I}{2C_{II}}\right) \quad \text{(A-12)}$$

Assuming that this system follows ideal behavior ($f_I = f_{II} = 1$), eq A-12 becomes

$$J_{CO_2} = -\frac{\sigma_1 \sigma_2 RT}{8(\sigma_1 + \sigma_2)F^2}\left(\frac{4}{C_I} - \frac{1}{C_{II}}\right)\nabla C_I \quad \text{(A-13)}$$

Concentration (C_i) values and their gradient can be calculated using the ideal gas law:

$$C_I = \frac{2}{3}\left(\frac{P_t}{RT}\right)$$

$$C_{II} = \frac{1}{3}\left(\frac{P_t}{RT}\right)$$

where

$$P_t = P_{CO_2} + P_{CO} = P_I + P_{II}$$

$$P_I = \frac{2}{3}P_t$$

$$P_{II} = \frac{1}{3}P_t$$

and

$$\nabla C_1 = \left(\frac{1}{RT}\right)\left(\frac{dP_{CO_2}}{dL}\right)$$

The subscripts "CO_2" and "CO" represent partial properties, whereas the subscript "t" represents total properties.
Inserting the concentration and their gradient into eq A-13 yields

$$J_{CO_2} = -\frac{\sigma_1\sigma_2 RT}{8(\sigma_1+\sigma_2)F^2}\left(\frac{3}{P_t}\right)\frac{dP_{CO_2}}{dL} \qquad \text{(A-14)}$$

Integrating eq A-14 for one-dimensional system for L (from 0 to L) and P_{CO2} (from P_1, feed side to P_2, permeate side):

$$\int_0^L J_{CO_2}\,dL = -\int_{P_1}^{P_2}\frac{3\sigma_1\sigma_2 RT}{8(\sigma_1+\sigma_2)F^2}d\ln P_{CO_2} \qquad \text{(A-15)}$$

$$\therefore J_{CO_2} = -\frac{3RT}{8F^2L}\int_{P_1}^{P_2}\frac{\sigma_1\sigma_2}{(\sigma_1+\sigma_2)}d\ln P_{CO_2} \qquad \text{(A-16)}$$

eq A-16 becomes eq. (3) in the main text.